

ROLE OF POLY (PROPYLENE FUMARATE) (PPF) BASED SCAFFOLDS IN BONE
REGENERATION



by
Begüm Okutan

Submitted to Graduate School of Natural and Applied Sciences
in Partial Fulfillment of the Requirements
for the Degree of Master of Science in
Biotechnology

Yeditepe University
2018

ROLE OF POLY (PROPYLENE FUMARATE) (PPF) BASED SCAFFOLDS IN BONE
REGENERATION

APPROVED BY:

Prof. Dr. Gamze Torun Köse
(Thesis Supervisor)



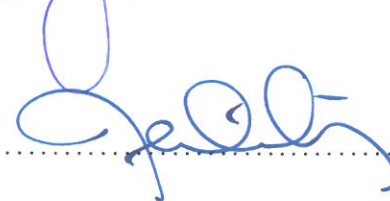
Assoc. Prof. Dr. Erde Can
(Thesis Co-supervisor)



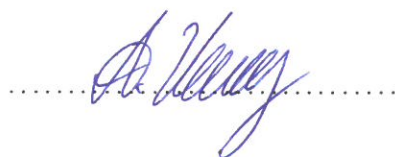
Prof. Dr. Ebru Toksoy Öner



Assoc. Prof. Dr. Fatma Neşe Kök



Assist. Prof. Dr. Andrew John Harvey



DATE OF APPROVAL:/....../2018



To my beloved grandparents...

ACKNOWLEDGEMENTS

Firstly, I would like to thank my supervisor Prof. Gamze Torun Köse for her guidance, support, advice, and encouragement for this project. I especially appreciate the optimism, kindness, and motivation she provided throughout my undergraduate and graduate years. I would also like to thank to my co-advisor Assoc. Prof. Erde Can for giving me the opportunity to study on this project.

I would like to thank to Görkem Cemali for her assistance and advices which made me obtain good results without dealing with many problems and complete my experiments in a better way. I would also like to thank YUTEG members Dr. Görke Gürel Peközer, Dr. Ayşe Ceren Çalikoğlu, Dr. Ayşe İrem Kanneçi, Dr. Ayşegül Atasoy, Dr. Özge Acar, Nergis Abay, and Ezgi İrem Bektaş for their friendship, suggestions, encouragement, and help throughout my undergraduate and graduate works.

I am especially indebted to my dear friends, Çağla Görkem Eroğlu, Bahar Hazal Yalçinkaya, Gizem Özan, and Neslihan Kayra since they always supported me morally and tried to help me in any possible subject during my laboratory work and while I was writing my thesis.

Last but not least, I am grateful to my parents, Bahadır Okutan and Fatma Gül Okutan, and also my lovely sister Bengü for their endless love, trust, support, understanding, and patience.

ABSTRACT

ROLE OF POLY (PROPYLENE FUMARATE) (PPF) BASED SCAFFOLDS IN BONE REGENERATION

In tissue engineering applications, biomaterials have significant roles to support cells and promote cell growth, proliferation, and differentiation. The initial response of the cells to the scaffold directly affects the cell adhesion, growth, proliferation and differentiation. Therefore, biomaterials should be biocompatible, biodegradable, and have good mechanical properties. In recent years, natural polyesters and fumaric acid based polyesters have attracted a lot of interest in bone tissue engineering (BTE) applications because of their superior biocompatibility, biodegradability, and mechanical property. One of the extensively investigated polyester is poly (propylene fumarate) (PPF), an unsaturated linear polyester, which can be modified or crosslinked through its carbon-carbon double bonds and used in different composites in tissue engineering applications.

The purpose of this study was to investigate the role of PPF based novel scaffolds in bone regeneration. For this purpose, synthesized PPF polymers were cured in the presence of two phosphonic acid based monomers; vinyl phosphonic acid (VPA) and vinyl phosphonic acid diethyl ester (VPES) at different concentrations with two methods: cure at body temperature (BT) in the presence of a suitable initiator and catalyst and UV cure at body temperature. Also, PPF/VPES based scaffolds were cured at different concentrations of beta-tricalcium phosphate (β -TCP, 0 per cent, 5 per cent, 10 per cent, 15 per cent, 20 per cent) at BT in order to support osteogenesis. Following analyses were carried out to indicate the osteoblast activity in the presence of this novel biomaterial. The morphology of the cell seeded scaffolds was analyzed by scanning electron microscopy (SEM). Biocompatibility, osteoblast cell attachment, proliferation, mineralization, alkaline phosphatase, and osteocalcin activities were evaluated. All experiments demonstrated that UV-cured and BT-cured PPF based scaffolds and its composites with β -TCP were biocompatible and promoted osteoblast cell attachment, proliferation, growth, and differentiation. Therefore, significant potential of the usage of crosslinked PPF/VPA and PPF/VPES based scaffolds in BTE applications was shown in this study.

ÖZET

POLİ (PROPİLEN FUMARAT) (PPF) BAZLI DOKU İSKELELERİNİN KEMİK REJENERASYONUNDAKİ ROLÜ

Doku mühendisliği uygulamalarında biyomateryaller, hücrelerin büyümesi, çoğalması ve farklılaşmasında önemli rol oynar. Hücrelerin biyomateryaller ile ilk etkileşimi, hücre tutunmasını, büyümesini, çoğalmasını ve farklılaşmasını doğrudan etkiler. Bu nedenle, biyomateryaller biyolojik olarak uyumlu, biyobozunur, fiziksel ve kimyasal olarak biyolojik dokuyu taklit edebilen nitelikte olmalıdır. Son yıllarda, doğal polyesterler ve fumarik asit bazlı polyesterler, biyoyumluluk, biyobozunurluk ve mekanik özelliklerinin diğer polimerlere göre daha iyi olmasından dolayı kemik doku mühendisliği çalışmalarında yoğun ilgi çekmektedir. Kapsamlı olarak incelenen doymamış polyesterlerden biri olan polipropilen fumarat (PPF), karbon-karbon çift bağlarından dolayı çapraz bağlanabilir, kolayca modifiye edilebilir ve farklı kompozitler ile kemik doku mühendisliği çalışmalarında kullanılabilir.

Bu çalışmada, PPF bazlı doku iskelelerinin kemik rejenerasyonundaki rolü araştırılmıştır. Bu amaçla, sentezlenen PPF polimerleri iki fosfonik asit monomer; vinil fosfonik asit (VPA) ve vinil fosfonik asit di-etil esteri (VPES) varlığında farklı konsantrasyonlarda iki farklı metot kullanılarak kür edilmiştir: uygun radikal başlatıcı ve kataliz varlığında vücut sıcaklığında kür ve mor ötesi (UV) ışık altında oda sıcaklığında kür. Ayrıca, PPF/VPES bazlı iskeleler kemik doku oluşumunu desteklemek için farklı β -TCP konsantrasyonlarında (0, 5, 10, 15, 20) vücut sıcaklığında kür edilmiştir. Hazırlanan doku iskelelerinin üzerindeki hücrelerin morfolojik özellikleri taramalı elektron mikroskobu ile görüntülenmiştir. Daha sonra, osteoblast hücrelerinin hazırlanan doku iskeleleri ile biyoyumluluğu, mineralizasyon, alkalik fosfat ve osteokalsin aktiviteleri incelenmiştir. Tüm deneyler, UV ışık altında ve vücut sıcaklığında kürlenmiş PPF bazlı iskelelerin ve kompozitlerinin biyoyumlu olduğunu ve osteoblast hücrelerinin tutunmasını, çoğalmasını, büyümesini ve farklılaşmasını desteklediğini göstermektedir. Dolayısıyla, bu çalışmada, kemik doku mühendisliği uygulamalarında kullanılmak üzere üretilen çapraz bağlı PPF/VPA ve PPF/VPES bazlı doku iskelelerinin potansiyel kullanımını gösterilmiştir.

TABLE OF CONTENTS

ACKNOWLEDGEMENTS.....	iv
ABSTRACT.....	v
ÖZET	vi
LIST OF FIGURES	x
LIST OF TABLES.....	xii
LIST OF SYMBOLS/ABBREVIATIONS.....	xiii
1. INTRODUCTION.....	1
2. LITERATURE REVIEW	2
2.1. BONE ANATOMY AND PHYSIOLOGY	2
2.1.1. Osteoblasts	3
2.1.2. Osteocytes	4
2.1.3. Bone Lining Cells	4
2.1.4. Osteoclasts	5
2.2. BONE MODELING AND REMODELING.....	5
2.2.1. Alkaline Phosphatase	7
2.2.2. Osteocalcin.....	7
2.2.3. Osteopontin.....	7
2.2.4. Bone sialoprotein	8
2.2.5. Osteonectin	8
2.3. BONE HEALING	8
2.4. BONE TISSUE ENGINEERING	9
2.4.1. Cell Sources as a Key Factor	11
2.4.1.1. Embryonic Stem Cells.....	11
2.4.1.2. Mesenchymal Stem Cells	12
2.4.1.3. Bone Marrow Stromal Cells.....	12
2.4.1.4. Multipotent Adipose-Derived Stromal Cells.....	12
2.4.1.5. Non-osteogenic Cells (Vascular Cells)	13
2.4.2. Growth Factors as a Key Factor	13
2.4.3. Scaffolds as a Key Factor	15

2.4.3.1.	Metals as a Scaffold.....	16
2.4.3.2.	Ceramics as a Scaffold	17
2.4.3.3.	Polymer as a Scaffold.....	18
2.4.3.4.	Poly(propylene fumarate).....	19
2.4.3.5.	Polyvinyl phosphonic acid (PVPA) and derivatives	21
2.5.	AIM OF THE STUDY	22
3.	MATERIALS AND METHODS	24
3.1.	MATERIALS	24
3.2.	METHODS.....	24
3.2.1.	Preparation of PPF Based Scaffolds	24
3.2.2.	Osteoblast Cell Culture.....	25
3.2.3.	<i>In vitro</i> Cell-Biomaterial Interaction Studies.....	25
3.2.3.1.	Scanning Electron Microscopy (SEM).....	26
3.2.3.2.	Cell proliferation-MTS assay	26
3.2.3.3.	von Kossa Staining	26
3.2.3.4.	Alkaline Phosphatase.....	27
3.2.3.5.	Osteocalcin Assay	27
3.2.4.	Statistical Analysis.....	28
4.	RESULTS.....	29
4.1.	<i>IN-VITRO</i> CELL-BIOMATERIAL INTERACTION	31
4.1.1.	Scanning Electron Microscopy (SEM) Analysis	31
4.1.2.	Cell proliferation-MTS assay.....	37
4.1.3.	von Kossa Staining	40
4.1.4.	Alkaline Phosphatase Assay	44
4.1.5.	Osteocalcin Assay.....	47
5.	DISCUSSION.....	50
6.	CONCLUSION	55
7.	FUTURE PROSPECTS.....	56
	REFERENCES	57
	APPENDIX A.....	70

APPENDIX B.....71



LIST OF FIGURES

Figure 2.1. Schematic drawing of bone morphology.....	3
Figure 2.2. The major products and properties of osteoblast.....	4
Figure 2.3. The illustration of four stages of bone healing.....	9
Figure 2.4. The key stages of tissue engineering.....	11
Figure 2.5. Chemical structure of poly(propylene fumarate).....	19
Figure 4.1. UV-cured PPF/VPES (70/30) polymers.....	29
Figure 4.2. UV-cured PPF/VPA (70/30) polymers.....	30
Figure 4.3. BT-cured PPF/VPES polymers.....	30
Figure 4.4. SEM images of UV-cured PPF/VPA (70/30) samples.....	32
Figure 4.5. SEM images of UV-cured PPF/VPES (70/30) samples.....	33
Figure 4.6. SEM images of BT-cured PPF/VPES (70/30) samples.....	35
Figure 4.7. SEM images of BT-cured PPF/VPES (70/30) composites.....	36
Figure 4.8. Proliferation of HOOb cells on UV-cured PPF/VPA (70/30) and PPF/VPES (70/30) samples with different BAPO concentrations.....	38
Figure 4.9. Proliferation of HOOb cells on BT-cured PPF/VPES (70/30) samples and its composites with different β -TCP ratios.....	39

Figure 4.10. von Kossa staining of UV-cured PPF/VPA (70/30) polymers	41
Figure 4.11. von Kossa staining of BT-cured PPF/VPES (70/30) polymers	43
Figure 4.12. ALP activity of HOB cells on UV-cured PPF/VPA (70/30) and PPF/VPES (70/30) samples with different BAPO concentrations... ..	45
Figure 4.13. ALP activity of HOB cells on BT-cured PPF/VPES (70/30) samples and its composites with different β -TCP ratios	46
Figure 4.14. OC activity of HOB cells on UV-cured PPF/VPA (70/30) and PPF/VPES (70/30) samples with different BAPO concentrations.....	48
Figure 4.15. OC activity of HOB cells on BT-cured PPF/VPES (70/30) samples and its composites with different β -TCP ratios.	49

LIST OF TABLES

Table 2.1. The most commonly used growth factors in BTE.....	14
Table 4.1. von Kossa staining results of UV-cured PPF/VPA and PPF/VPES samples according to ColorPic software.....	42
Table 4.2. von Kossa staining results of BT-cured PPF/VPES samples and composites according to ColorPic software	44



LIST OF SYMBOLS/ABBREVIATIONS

ASCs	Adipose derived stromal cells
ALP	Alkaline phosphatase
BCLs	Bone lining cells
BAPO	Bisacylphosphine oxide
BMP	Bone morphogenic protein
BMSCs	Bone marrow stromal stem cells
BSP	Bone sialoprotein
BP	Benzoyl peroxide
BRU	Bone remodeling units
BT	Body temperature
BTE	Bone tissue engineering
DMEM	Dulbecco's Minimal Eagle Medium
DMT	Dimethyltoluene
ECM	Extracellular matrix
FBS	Fetal bovine serum
FGF	Fibroblast growth factor
HA	Hydroxyapatite
HCA	Hydroxyl carbonate apatite
HOb	Human osteoblast
HSCs	Hematopoietic stem cells
IGF	Insulin-like growth factor
MMA	Methyl methacrylate
MSCs	Mesencymal stem cells
NVP	N-vinyl pyrrolidinone
OC	Osteocalcin
OPN	Osteopontin
OSN	Osteonectin
PBS	Phosphate buffered saline
PDGF	Platelet derived growth factor
PPF	Poly(propylene)fumarate

SEM	Scanning electron microscopy
TCP	Tricalcium phosphate
TE	Tissue engineering
TGF- β	Transforming growth factor beta
UV	Ultraviole
VPA	Vinyl phosphonic acid
VPES	Vinyl phosphonic acid diethyl ester
PVPA	Polyvinyl phosphonic acid



1. INTRODUCTION

Bone is a complex living tissue which undergoes constant turnover throughout life. Even though, bone tissue has an ability to heal itself, the repair of traumatic injury, critical sized defects, infection, or diseases can be more difficult. Generally, these bone defects are repaired by using bone grafting. However, bone grafts (i.e. cements, metal rods, plates and screws) have high complication rate due to risk of immunogenic reactions, infections, and transmission of diseases.

BTE field holds a central role to solve the problem of bone healing. This field combines cells for regenerating the bone tissue, growth factors for cell functioning, and biomaterials for temporary scaffolds. Within the field of BTE, it is important to understand fundamentals of bone biology, bone engineering strategies, and design of BTE construct.

One of the key factor for BTE strategies is to choose an appropriate biomaterial which should be biocompatible, biodegradable for allowing native tissue integration, physically and chemically biomimetic, and also have an ability of carrying bioactive molecules which accelerates extracellular matrix (ECM) production, tissue integration or drugs for preventing undesired biological response. Although, different biomaterials including metals, natural polymers, synthetic polymers, and ceramics have been used for their potential as being a scaffold, polymers have become the principal biomaterial because of their tunable physiochemical features, biocompatibility, and controllable degradability.

Since, bone is obviously important part of the body especially along with bone diseases such as osteoporosis, osteomalacia, bone cancers, orthopedic surgeries, and traumatic injury, bone regeneration has a crucial role in healing of these diseases. Therefore, the designing the biomaterial which can fulfill all the desired requirements for bone regeneration is the first crucial step in BTE applications.

2. LITERATURE REVIEW

2.1. BONE ANATOMY AND PHYSIOLOGY

Bone is a rigid, complex, and highly specialized tissue that takes part in a variety of critical functions in human physiology. Mechanical function covers mainly protection and support of critical organs and movement of muscles and tendons with interacting them. It is also a metabolic reservoir of minerals (i.e., calcium, phosphorus) and multiple progenitor cells to maintain homeostosis and regulate blood pH [1, 2].

Generally, bone is classified in two types in terms of macroscopic level: cortical bone and cancellous or trabecular bone (Figure 2.1.). Cortical bone and trabecular bone constitutes the 80 per cent and 20 per cent of bone respectively [3]. Compact bone has a 5-10 per cent of porosity and seems like a solid mass whereas trabecular bone has a porosity of 50-95 per cent [4]. The main constituents of the cortical bone are osteons that are the cells strengthening and directing the length of the long bones. Osteons form from frail layers of the lamellae which preserve the internal core of the compact bone. This mineralized bone type has a 10-40 GPa of elastic modulus and 90-140 MPa of yield strength [5]. Therefore, it is responsible from maintaining mechanical and protective requirements of the skeleton. On the other hand, cancellous bone is less dense but highly porous. It does not include blood vessels in trabeculae. The red bone marrow fills the spaces between trabeculae and supplies nutrients and oxygen to the osteocytes.

On a microscopic level, bone structure includes wide range of cell types and bone matrix that consists of inorganic and organic components. In terms of organic components, 95 per cent of bone matrix is composed of collagen (mostly type I collagen) and the rest of 5 per cent is proteoglycans aggregates (i.e. proteoglycans, hyaluronic acid) and non-collagenous proteins such as osteocalcin (OC), osteopontin (OPN), and biglycan [6, 7]. However, the main component of bone matrix is mineral especially calcium phosphate ($\text{Ca}_3(\text{PO}_4)_2$) and hydroxyapatite ($\text{Ca}_{10}(\text{PO}_4)_6(\text{OH})_2$). Combination of these minerals and collagen fibers in the ECM enhances mechanical properties (i.e. hardness, compressive and tensile strength) to bone [8].

In addition, bone cells comprises of 2 per cent of bone mass and interaction of these different cell types provides dynamic tissue properties to bone [9]. Bone cell types are divided into 2 main groups which are cells from osteoblast lineage (i.e. osteoprogenitor cell, osteoblast, and osteocyte) and monocyte-macrophage-osteoclast lineage [10].

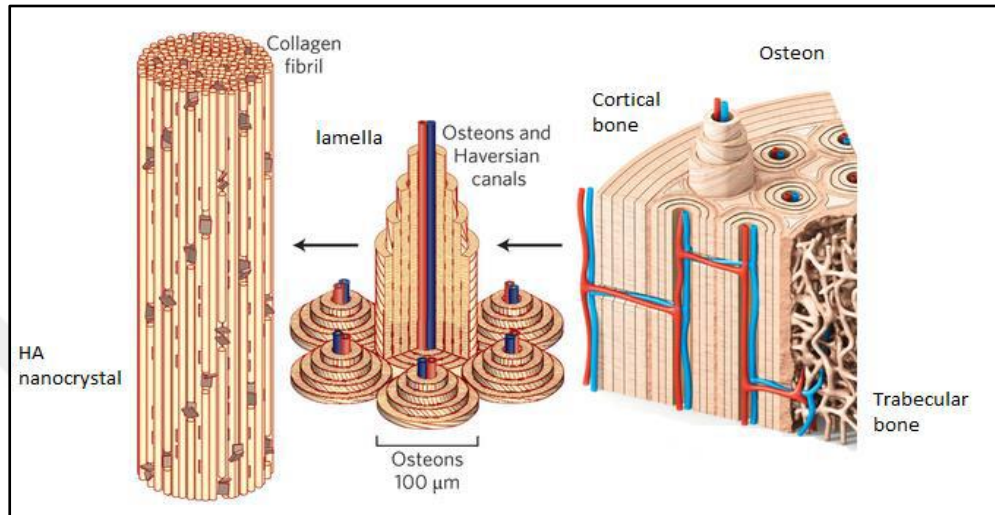


Figure 2.1. Schematic drawing of bone morphology [11]

2.1.1. Osteoblasts

Osteoblasts are epithelial-like immature bone cells with cuboidal shape. They tend to form a monolayer on the bone surface. This cell type derives from mesenchymal stem cells (MSCs) or bone marrow stromal cells (BMSc). First, they proliferate and differentiate into preosteoblasts, and then become mature osteoblasts. These highly polarized osteoblasts secrete type I collagen, alkaline phosphatase, non-collagenous proteins (i.e. OC, OSP, and BSP, bone sialoprotein), and other inorganic compounds of the ECM during osteogenesis. Also, vitamin D₃ plays a role in osteocalcin expression, bone mineralization, and preservation of calcium and phosphate in bone (Figure 2.2). Therefore, generally they can be found on newly formed and unmineralized tissue. Also, these secreted proteins have a responsibility to regulate bone cell activity, mineral storage, and turnover [3]. Furthermore, osteoprotegerin, receptor activator of nuclear factor κ B ligand, and macrophage-colony stimulating factor have responsibility to organize the differentiation of osteoclasts (Figure 2.2). Osteoblasts not only deposit osteoid but also initiate and regulate the subsequent

mineralization of osteoid and after sufficient deposition, they can decrease their metabolism and differentiate into osteocytes.

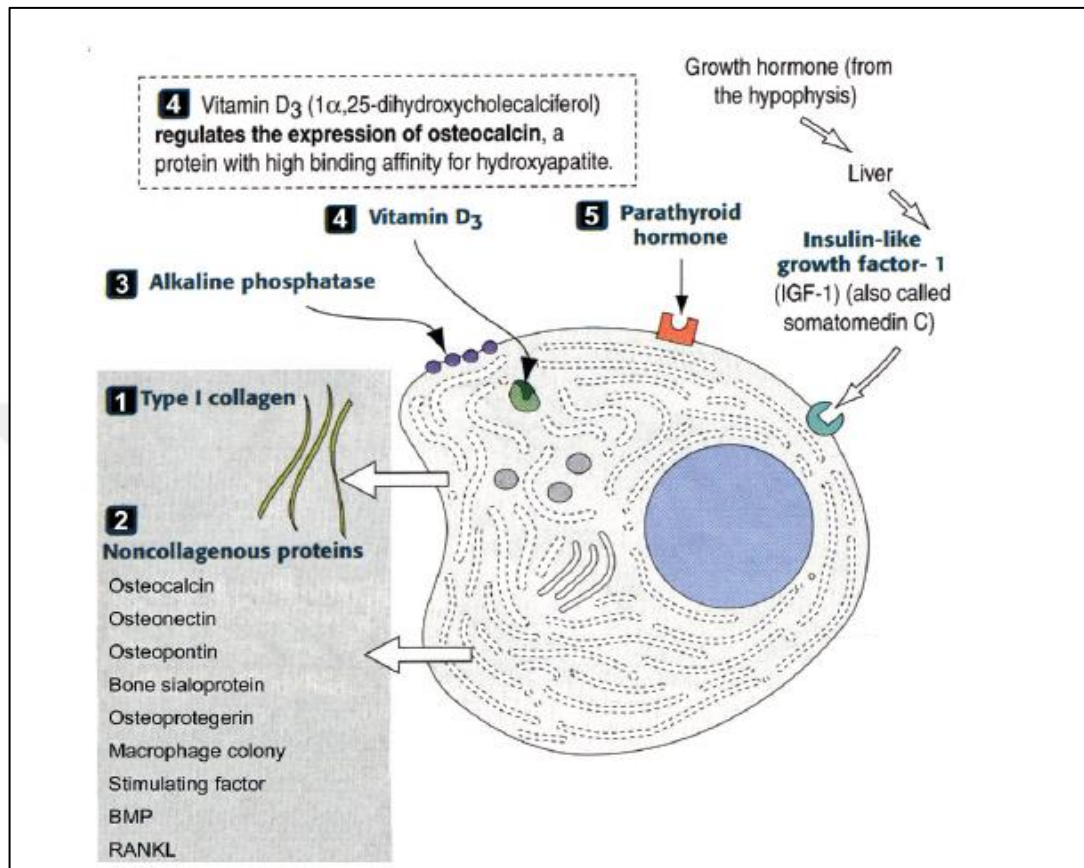


Figure 2.2. The major products and properties of osteoblast [10]

2.1.2. Osteocytes

Osteocytes that are the most abundant cell type in the bone have a stellate shape residing in lacunae between layers of the mineralized bone matrix. They have a role in maintenance and remodeling of bone matrix and mineral homeostasis. Their filopodial processes provide an interaction with each other and also with the bone surface [12].

2.1.3. Bone Lining Cells

Bone lining cells (BCLs) present on the surface of the bones. They are quiescent osteoblasts with a spindle shape. There are some debates about functionality of BCLs.

Some researchers have considered that BCLs have an important role in hematopoiesis and marrow stromal system whereas others claim that BCLs support mineral homeostasis [12, 13].

2.1.4. Osteoclasts

Osteoclasts which is the highly polarized bone cells, comprises of the monocyte-macrophage progenitor cell lineage in the bone marrow. Monocytes are the precursor cells of osteoclasts and when they reach to bone via circulating blood, they fuse into multi-nucleated cells to generate osteoclasts. Therefore, osteoclasts are large (approximately 100-200 μm) and multi-nucleated cells with a responsibility of bone resorption. Also, their shapes are varying from flat to round according to the phase of the bone resorption cycle [14].

Osteoclasts have a ruffled border and clear zone plasma membrane areas. Clear zone, also called as a sealing zone, encloses the ruffled border area where osteoclasts secrete HCl and collagenase for bone resorption. As a consequence of this acid secretion, hydroxyapatite crystals dissolve and mineralized ECM is formed. On the other hand, collagenases and other enzymes destroy the collagen matrix to protect hydroxyapatite crystals [15, 16, 17]. Calcitonin, vitamin D₃, and regulatory molecules are the main factors to regulate osteoclast activity.

2.2. BONE MODELING AND REMODELING

Bone modeling is a dynamic process of bone shape and reshaped alteration through the independent interactions of osteoblasts and osteoclasts. This process is responsible for skeletal development, growth, and so shaping of bones and their movement. The turnover rate of the skeleton is approximately 100 per cent in the first year of life, it reduces 10 per cent per year until early teens, and then it decreases dramatically in time [18, 19].

While bone modeling is an independent process, bone remodeling covers dependent and coordinated interactions of osteoblasts and osteoclasts and this coordinated interactions continue throughout the human's life. Approximately 1 million of bone remodeling units

(BRUs) can actively take part in bone turnover process [20]. In adult skeleton, BRU is composed of osteoblasts, osteoclasts, nerve supply, vascular capillary, and connective tissue. The purpose of this process is to maintain calcium homeostasis, acid- base balance, replace the old and damaged bones with new bone [21].

Bone remodeling has four phases mainly including the osteoblast and osteoclast activity. Activation phase is called as osteoclasts recruitment. Second phase is the resorption phase that includes bone resorption by osteoclasts. This phase is followed by reversal phase. Briefly, this phase contains apoptosis of osteoclasts and recruitment of osteoblasts. Formation phase is the final phase in which bone matrix is formed by osteoblasts [20]. In detail, bone remodeling is initiated by the activation of preosteoclastic cells in bone marrow. Previously described bone lining cells (inactive) release interleukin-1 (IL-1), parathyroid hormone, and cytokines and this leads to migration of preosteoclastic cells to bone surface. Then, preosteoclastic cells turn into osteoclasts and develop a ruffle border. Mature osteoclasts fill the spaces of bone matrix surface by secreting H^+ ions and cathepsin. In resorption phase, osteoclasts resorb the Ca^{2+} on the surface of cancellous and cortical bone. Parathyroid hormone not only stimulates osteoclasts to resorb bone but also stimulates the osteoblasts to produce IL-6 [22, 23]. In addition, IL-1 activates the preosteoclastic cells and then these cells produce channels for the growth of blood capillaries. By the help of osteoblasts, blood flows to the bone from these channels [23, 24]. In the last phase of the bone remodeling, type I collagen and bone matrix proteins are secreted by osteoblasts. Polymerized collagen generates triple stranded fibers for osteoid formation. Thicker osteoid initiates the mineralization process (precipitation of Ca^{2+} and PO_4^{3-} ions) and it provides the formation of hydroxyapatite (HA) crystals. Finally, osteoblasts which are trapped into bone matrix by HA mature into osteocytes [25].

Although there are no produced bone specific markers during the bone modeling and remodeling process, bone includes a number of specific proteins at different concentrations. These specific bone markers are ALP, OC, OPN, osteonectin (OSN), collagen type I, BSP, and bone morphogenic proteins (BMP).

2.2.1. Alkaline Phosphatase

ALP which is a cell surface protein, is the widely preferred marker for bone formation. It can bind to the plasma membrane through phosphatidylinositol phospholipid complexes. Its expression in blood is highly correlated with bone formation. However, it is also expressed by liver, kidney, placenta, intestine, and other tissues [26]. The exact role of ALP has not been understood yet but some studies suggested that ALP has an important role in skeletal mineralization. It hydrolyzes a phosphate ester and this situation leads to increase local concentration of inorganic phosphate which then provides formation of HA. Others suggested that ALP can facilitate formation of calcium phosphate precipitation by acting as a transporter for inorganic phosphate to bind calcium [27, 28].

2.2.2. Osteocalcin

Osteocalcin is non-collagenous bone protein which can also be named as bone γ -carboxy glutamic acid protein (bone gla protein). It is also an osteoblast specific secreted protein and a mid-marker of bone formation. OC includes the vitamin K dependent Ca^{2+} binding amino acid. As a result, it has a very high affinity to Ca^{2+} ions. Generally, osteoblasts, odontoblasts, and hypertrophic chondrocytes synthesize this protein and they are deposited in the ECM. Serum osteocalcin level is associated with the rate of bone formation and it has a greater sensitivity than ALP in the detection of osteoblast activity [29].

2.2.3. Osteopontin

OPN is a phosphorylated glycoprotein that is synthesized by various cells such as osteoblasts, preosteoblasts, and osteocytes. It has a critical role in cell activation, mineralization of bone, inhibition of calcification, coordination of immune cell function, tumor cell phenotype, and. In bone mineralization, it promotes the attachment and spread of osteoblasts through the ECM and anchors osteoclasts to inhibit the formation of HA [30]. In addition, studies indicated that OPN is found in larger amounts at the borders of growth plates (in growing bone) and injured site (between healing and native bone). It is also detected between the implant and native bone [31].

2.2.4. Bone sialoprotein

BSP is a phosphorylated and glycosylated protein. It is not only found in mature osteoblasts and osteocytes but also found in chondrocytes, cartilage, and osteoclasts. It is responsible for mediating cell attachment to ECM [32]. Also, it has a high affinity to Ca^{2+} ions.

2.2.5. Osteonectin

This glycoprotein is also known as secreted protein acidic (SPARC) and rich in cysteine. Osteoblasts, vascular smooth muscle cells, endothelial cells, and chondrocytes are some of the cell types that express OSN [33]. It was demonstrated that OSN mediates binding of growth factors to cells and controls cellular progression [34, 35]. Collagen Type I constitutes 95 per cent of the ECM so it is the most abundant protein found in bone. It also exists in tendons, ligaments, and skin. This protein is involved in the mechanical properties of bone because of its triple helix structure [36].

2.3. BONE HEALING

The main aspects of bone healing combine skeletal development and growth. This process constitutes from four stages that are inflammation, formation of soft callus, formation of hard callus, and remodeling (Figure 2.3). Local soft tissue integrity is disrupted in bone defects which causes bleeding within the defect site and the development of a hematoma. The beginning of inflammation process is not specific for tissues. Accordingly, inflammation is described by an up-regulation of inflammatory mediators [37]. Platelets, macrophages, and inflammatory cells play a role in the site of injury to strive against infection. They can secrete cytokines and growth factors which coordinate the cellular response. Also, these cells promote clotting and then, new capillaries are formed into this clot by endothelial cells [38]. After ossification cartilaginous template is formed providing a semi-rigid support to the fracture. Chondrocytes and fibroblasts have a specific function for the synthesis of the cartilaginous matrix that is a temporary bridge between the damaged fragments. Furthermore, growth factors regulate fibroblast proliferation,

mineralization of cartilaginous matrix, and vascularization. Hard callus formation is regulated by osteoblasts that are differentiated from osteoprogenitor cells. Osteoblasts produce mineralized bone matrix resulting in degradation of unstable soft tissue. On the other hand, revascularization is supported by osteoblasts. The last step of bone healing is bone remodeling involving replacement of hard tissue with new cortical or trabecular bone. As it was mentioned in previous part, osteoclasts resorb the surface of the bone with secreting acid and proteinases and osteoblasts form new bone and secrete cytokines to affect osteoclast behavior in this process [32].

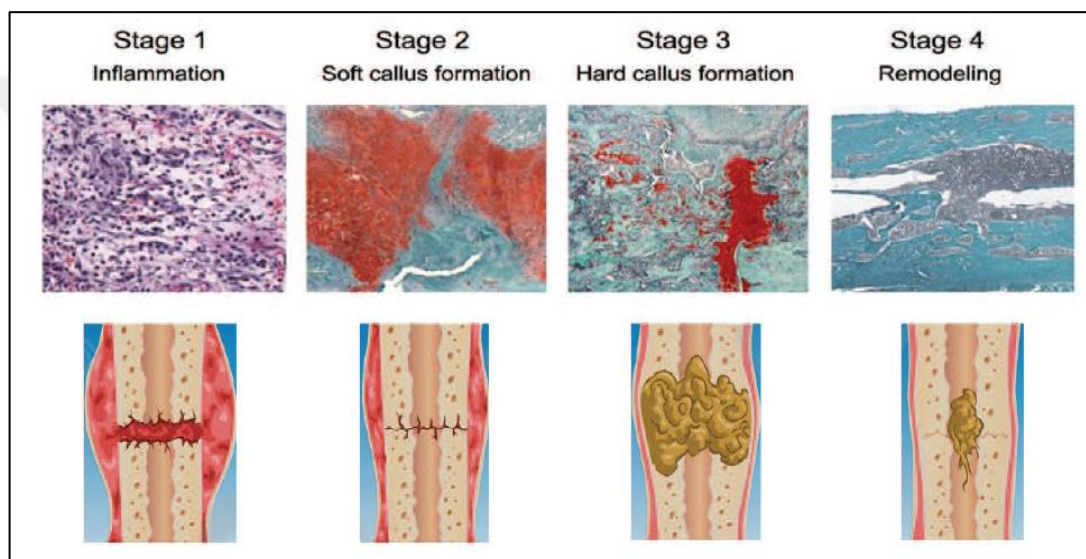


Figure 2.3. The illustration of four stages of bone healing [37]

2.4. BONE TISSUE ENGINEERING

As it has been mentioned before, bone is a dynamic tissue which is constantly remodeling itself [39]. In the case of non-unions, critical sized defects or traumatic injuries, its self-repair mechanism is limited. In these situations bone grafting are used to support and enhance the biological repair. Today, the most commonly used bone grafting is autologous bone grafting and the second one is the allogenic bone grafting [39, 40]. Autografts, allografts, and synthetic biomaterials constitute 58 per cent, 34 per cent, and 8 per cent of the world market for bone grafting, respectively [41, 42]. However, the risk of infection, chronic pain, and disability can be observed in autologous bone grafting [43, 44]. Similarly, allogenic bone grafting can lead to immunogenic reactions, transmission of

diseases, and infection [45]. Therefore, tissue engineering (TE) is a considerable option to treat critical sized defects. TE was initially described as an interdisciplinary field that combines different principles such as engineering, medicine, biochemistry, and biology. Therefore, TE applications develop permanent or temporary functional substitutes for restoring, maintaining, and improving tissue function [46]. In addition, the development of these functional substitutes or tissues are achieved by using biomaterials, growth factors, and cells that are the three critical strategies of TE (Figure 2.4).

BTE is an important branch of TE that covers the multiple strategies containing development of scaffolds, cell transplantation, gene therapy, stem cell therapy, and growth factor delivery that are alternative to bone grafting procedures. Even though these strategies are generally used in combination, two of them are considered as the commonly preferred approaches: i) MSCs are isolated, improved *ex vivo*, transferred onto a developed biomaterial permitting to produce ECM on the biomaterial in controlled specific culture conditions, and implanted into the defected site, ii) An acellular scaffold is implanted just after injury/bone removal [8].

Osteogenic progenitor cells, an osteoconductive biomaterials, and osteoinductive growth factors are the important constituents for BTE [47]. Osteoconductive biomaterial provides the required atmosphere for osteogenic progenitor cells to generate new tissue and osteoinductive growth factors and they promote bone tissue regeneration and provide guidance for the desired differentiation pathways [48].

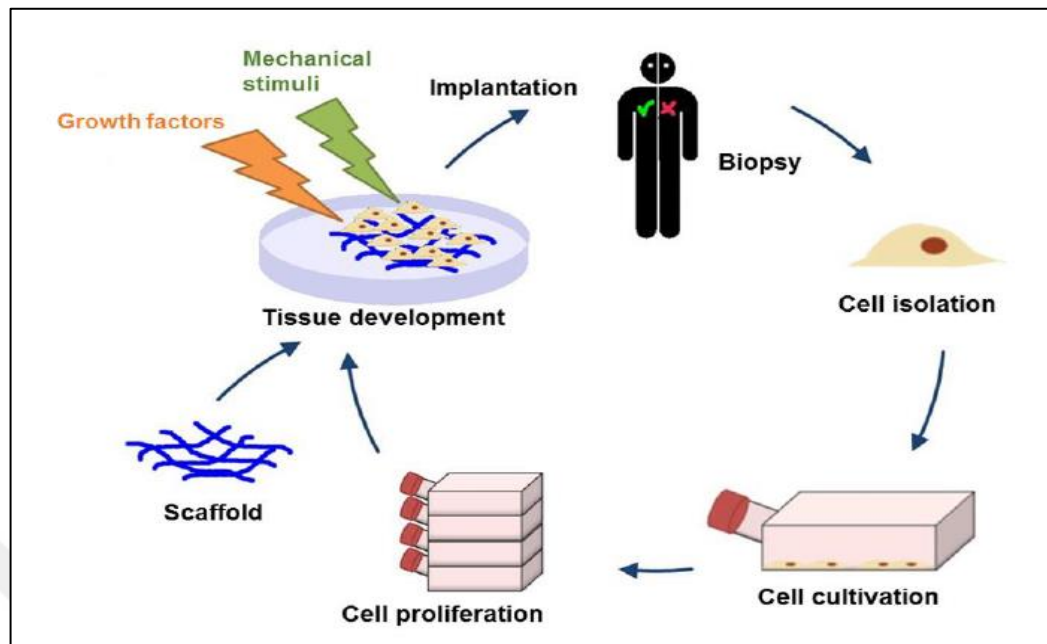


Figure 2.4. The key stages of tissue engineering [49]

2.4.1. Cell Sources as a Key Factor

As it was mentioned in previous parts, bone includes a various cell types such as osteoblasts, preosteoblasts, osteocytes, osteoclasts, chondroblasts, and marrow cells. However, there are limited cell sources to be used in BTE applications. These cell sources are autologous, allogenic, and xenogenic [50]. Considering their isolation and expansion efficiency, bone formation capacity, and immunologic response autologous cells are the most commonly used osteogenic constructs [51].

2.4.1.1. Embryonic Stem Cells

Embryonic stem cells are pluripotent stem cells which are able to differentiate into any type of cell. They can be cultured from fetal tissue but its human blastocyst's origin can be resulted in ethical issues [52]. It was indicated that derived osteoblast lineage cells are capable of forming mineralized tissue both *in vitro* and *in vivo*. Although, growth factors are generally used to direct the differentiation of a specific cell type, differentiated cells can be heterogeneous.

2.4.1.2. Mesenchymal Stem Cells

MSCs that are non-hematopoietic stem cells (HSCs) are derived from bone marrow. They are divided in symmetric and asymmetric cell division. In asymmetric stem cell divisions, one daughter cell possesses a stem cell characters, and the other one is differentiated. In symmetric cell division, each stem cells divides into two identical daughter cells. Therefore, they can maintain their stem cell characteristics when one stem cell divides into two [53]. They have an ability to differentiate into all cell types of the tissues or organs (i.e. osteoblasts, chondrocytes, adipocytes, myoblast) where they were originally harvested. Apart from this, they can support hematopoiesis and improve the engraftment of HSCs. Although MSCs are significant cell source for BTE, there are some challenges that are related to differentiation potential. They can tend to lose the frequency and differentiation potential according to their age. Therefore, they have different rate of proliferation and growth depending on their source and number of the culture passages [54, 55].

2.4.1.3. Bone Marrow Stromal Cells

BMSCs are the stem/progenitor cells of skeletal tissues. Similar to MSCs, BMSCs can be cell types varying from fibroblast-like spindle shaped cells to large flat cells under suitable conditions. BMSCs are rapidly adherent and clonogenic, so they are easily cultured and expanded in large numbers [56].

2.4.1.4. Multipotent Adipose-Derived Stromal Cells

Adipose derived stromal cells (ASCs) are another alternative cell type. ASCs have comparable morphology, differentiation capacity, and phenotype with MSCs so they can be used for skeletal regenerative medicine [57]. ASCs are easily obtained with excised surgical specimens or lipoaspirates [58].

2.4.1.5. *Non-osteogenic Cells (Vascular Cells)*

Bone is a highly vascularized tissue to supply nutrients, oxygen and also removes waste products. Accordingly, for BTE applications, angiogenesis is one of the important things for maintenance of tissue-engineered constructs. The cellular and molecular interaction between bone cells and blood vessels should be enhanced for survival and integration of TE construct with native tissue. Endothelial cells are classified into tip cells and stalk cells according to their sites on the growing vascular sprout. Their responsibility is to provide framework for new vascular network. Furthermore, endothelial cells have no side effects when they are transplanted autologously. Therefore, they are most commonly used cell types which enhance angiogenesis and bone formation. Brandi et al. indicated the importance of vascularization in osteogenesis and fracture repair using *in vitro* and *in vivo* models [59]. Also, Wegner *et al.* has developed a system where osteoblasts were incorporated into endothelial cell spheroids for inducing endothelial cell differentiation and *in vitro* angiogenesis [60].

2.4.2. **Growth Factors as a Key Factor**

Growth factors are secreted proteins to induce proliferation and growth of cells. They can stimulate or inhibit cell adhesion, proliferation, migration, and differentiation by mediating the protein synthesis, other kinds of growth factors, and receptors [61]. Therefore, growth factors have a crucial effect on tissue formation and they are the essential constituents for BTE applications [62]. Osteoinductive growth factors promote the differentiation of precursor cell types into osteoblasts [60]. BMPs are one of the major growth factors found in bone. They are secreted by MSCs, osteoblasts, and chondroblasts. BMPs are dimeric molecules with a single sulfide bond and a member of transforming growth factor beta (TGF- β) superfamily. They are responsible for bone remodeling, fracture healing, angiogenesis, synthesis of ECM, MSC proliferation, and differentiation [63]. In clinical applications, BMP-2 and BMP-7 are commonly used members of BMP family [64]. Delivery of BMPs is achieved by using some strategies such as direct administration, scaffold-based delivery, and gene therapy [65].

TFG- β , insulin-like growth factor (IGF), platelet derived growth factor (PDGF), and fibroblast growth factor (FGF) are the other growth factors that have a central function in fracture healing [41]. The sources and functions of the most commonly used growth factors for BTE is summarized in Table 2.1.

In addition to growth factors, a number of osteoinductive chemical compounds can promote the differentiation of precursor cell types into osteogenic lineage. In contrast to growth factors, these chemicals are less labile and have longer half-life. Also, they can be produced in the laboratory and used *in vitro* cell culture studies for several days [65, 66].

Table 2.1. The most commonly used growth factors in BTE [67]

Growth factor	Source	Function
TGF- β	Platelets, ECM, cartilage matrix	Stimulation and proliferation of MSCs
BMP	Osteoprogenitor cells, osteoblasts, ECM	Promoting differentiation of MSCs into chondrocytes and osteoblasts, and also differentiation of osteoprogenitors into osteoblasts, influencing skeletal pattern formation
FGF	Macrophages, MSCs, chondrocytes, osteoblasts	Mitogenic for MSCs, chondrocytes and osteoblasts and induction of angiogenesis
IGF I-II	Bone matrix, osteoblasts, chondrocytes	Promoting proliferation and differentiation of osteoprogenitor cells
PDGF	Platelets, osteoblasts	Mitogenic for MSCs and osteoblasts; macrophage chemotaxis

Dexamethasone, calcitriol (1,25-dihydroxyvitamin D3), TAK-778, statins, and prostaglandin E are the most commonly used osteoinductive chemicals in BTE. Dexamethasone is generally used with L-ascorbic acid and β -glycerophosphate. Stabilization of the collagen triple helix is achieved by hydroxyproline whose formation highly depends on usage of L-ascorbic as a cofactor for the hydroxylation of proline. β -glycerophosphate is used as an inorganic phosphate sources and it has a role in matrix mineralization process. Calcitriol inhibits adipogenic differentiation and stimulates osteogenic differentiation and mineralization of stem cells which are obtained from bone marrow. TAK-778 is used as an inducer of osteogenesis and statins have a function in osteogenic differentiation. Lastly, prostaglandin E induces the proliferation and differentiation of bone marrow derived stem cells [65].

2.4.3. Scaffolds as a Key Factor

As it was mentioned, bone is divided into two parts as cortical and cancellous bone. Cortical bone has a very dense structure with 5-10 per cent of porosity. It can bear a compressive stress in the range of 0.2-2942 MPa. Also, it has an elastic moduli up to 17GPa. On the other hand, the porosity of cancellous bone is 50-90 per cent. Its compressive stress is in the range of 2-15 MPa and elastic moduli is 44 MPa [68, 69]. Furthermore, bone ECM provides physical support and guidance for cell attachments, migration, and differentiation. Also, it is a reservoir of growth factors and cytokines [70]. Therefore, one of the key components in TE applications is a biomaterial that is used to make a scaffold for mimicking bone's structure and functions. Ten major properties were described for the development of scaffold. The suitable scaffold should be biocompatible, biodegradable, highly porous. Degradation time of the scaffold should correspond with the healing or regeneration of the tissue. It should also promote the formation of ECM, contribute a conductive surface for initial cell attachment and allow the proper nutrient-waste diffusion. Additionally, designed scaffold system should have good mechanical properties [71].

Biocompatibility is the primary criteria for the development of suitable scaffold. It is defined as an ability to perform desired function without any undesired response in specific cell or tissue [72]. Therefore, the scaffold and its byproducts must not elicit immunological responses while performing its function.

The biodegradability and bioresorbability are also important features of the scaffold. The scaffold should degrade and be resorbed over time and the degradation rate of the ideal scaffold should be controllable. If degradation rate is too slow, it can inhibit new tissue function, and if it is too rapid, it cannot allow cells to form and remodel native matrix to replace the scaffold. Accordingly, scaffold should support initial cell growth, proliferation, differentiation, and migration and degrade with equivalent rate for the new ECM production. The degradation rate of the synthetic scaffolds strictly based on molecular weight, morphology, porosity, and crosslinking density of the biomaterial. Although, naturally derived biomaterials have generally enzymatic biodegradation, many synthetic biomaterials cannot degrade under physiological conditions and release acidic compounds [46].

Furthermore, the scaffold should be osteoconductive which is the ability of stimulating bone forming cells for the regeneration of bone tissue [51].

Porosity, pore size and interconnectivity of the porous network of the scaffold are the other considerations. Highly porous network supports tissue growth and vascularization. The minimum pore size of the scaffold should vary between 100 μm to 800 μm [73]. Lastly, the mechanical properties have a crucial impact on cell attachment and proliferation. The elasticity, toughness, and strength of the scaffold should match with the native tissue's properties. The chemical structure, crosslinking density, swelling capacity, and processing methods are the major features affecting the strength of the scaffold (i.e. cross-linked structures have higher mechanical strength). On the other hand, scaffold elasticity can affect the cell behavior. It was indicated that MSCs growing on different scaffolds with different elasticity differentiated into distinct lineages [74].

There are numbers of biomaterials that have been used for TE applications. Metals, ceramics, and polymers (natural polymers and synthetic polymers) are the main groups of the biomaterial types.

2.4.3.1. Metals as a Scaffold

Metals that are very suitable to form scaffold since they are biocompatible, strong, processable, and inexpensive were used firstly in 1890s for bone repair. Since that time metals and metal alloys have been used for stabilization during the bone healing [75]. However, their modulus is generally higher than that of bone and this situation prevents biodegradation, growth of native tissue and may trigger the stress shielding. This situation is commonly observed in hip replacements [76]. Titanium, stainless steel and cobalt-chromium are the most widely used materials. Stainless steel is used as surgical tools and implanted devices. 316L austenitic stainless steel is the most widely used stainless steel type which includes iron, chromium, nickel, magnesium, and molybdenum [77]. However, under some circumstances, extended exposure of nickel can be the reason of allergic reactions. Therefore, nickel-free stainless steels are more biocompatible biomaterials [78]. Moreover, titanium and its alloys have low elastic modulus and lower sheer stresses which makes them more desirable for BTE applications [79]. Titanium does not only have good mechanic properties for new bone formation, they are also inert and resistant to corrosion.

Recent researchers have focused on functionally graded material by using titanium and ceramic compositions. Titanium surface can be coated with HA, chemicals, and matrix proteins to improve osseointegration, cell growth, and healing time [76, 77].

2.4.3.2. *Ceramics as a Scaffold*

Ceramics are generally used for fracture repair in the form of solid pieces, porous scaffold, powders, granules, and injectable formulations. Although ceramics have good biocompatibility they have an insufficient mechanical properties. Therefore, they are generally used with polymers as composites. They are categorized into three main groups in terms of chemical reactivity [82]. Resorbable ceramics are the first synthetic materials and their chemical composition, shape, and crystal structure affect the rate of resorption which occurs after osteogenesis. Calcium-phosphate is the most widely used ceramics which are known to adhere to bone and encourages bone tissue formation. Hydroxyapatite (HA), $\text{Ca}_{10}(\text{PO}_4)_6(\text{OH})_2$, tricalcium phosphate (TCP), $\text{Ca}_3(\text{PO}_4)_2$, biphasic calcium phosphates and multiphasic bio-glasses are the most common types of calcium-phosphate materials. TCP and HA are the most commonly studied calcium phosphates. TCP constitutes monocalcium phosphate monohydrate, alpha tricalcium phosphate, and calcium carbonate and it can be either injected or directly applied to the bone defect [75]. HA is used for bone defects that require long term treatments since its degradation time is long. While HA has an ability to adhere directly to bone due to its composition and structure similarity with the native bone mineral, it has an insufficient mechanical strength and is used with degradable polymers [79, 80, 81]. Also, HA can be used with metal alloys for enhanced bone integration and adhesion [79]. Bioactive ceramics can form physical bond to bone and they have lower content of SiO_2 but have higher content of NaO_2 and CaO . Glass surfaces of these materials become very reactive when they are exposed to an aqueous medium. This situation leads to formation of hydroxyl carbonate apatite crystals (HCA) on the surface [82, 83]. HCA layer formation is important since it enhances the mechanical and compressive strength. Bioinert ceramics have the best mechanical strength and biocompatibility since these materials do not react with the native bone tissue. They consist of generally metal oxides. Alumina (Al_2O_3), zirconia (ZrO_2), and titania (TiO_2) are the best examples of metal oxides. Bioinert ceramics are commonly used for large bone defects because of their great compressive strength [84, 85, 86].

2.4.3.3. Polymer as a Scaffold

Polymeric scaffolds were firstly used in early 1980s and they are the most suitable biomaterials used in TE applications. Considering their biocompatibility, degradability, processability, and general versatility, polymers are attractive biomaterials in BTE. Their biocompatibility highly depends on their degradative byproducts, surface chemistry, and the method of the polymer's erosion. Polymers are categorized into 2 main groups according to their sources: natural and synthetic polymers [87].

Natural polymers are biocompatible since they can resemble the substances naturally occurring in the body and are degraded by naturally occurring enzymes after implantation. The main advantage of these polymers is that they include biofunctional molecules which can assist cell attachment, proliferation, and differentiation. On the other hand, their degradation rate cannot be controlled and they have weak mechanical strength. However, mechanical strength can be enhanced by cross-linking. Also, there are other disadvantages such as batch to batch alterations, scale-up difficulties, and immunological reactions. Natural polymers are divided into 2 main groups: polysaccharides and polypeptides. Agarose, alginate, HA, chitosan are the most widely used polysaccharides whereas collagen, gelatin, and silk are the most widely preferred polypeptides in BTE applications [88].

Synthetic polymers are easily manufactured in large quantities and their physical properties (i.e. molecular weight, molecular structure) are easily controlled compared to natural polymers [89]. Structure of the synthetic polymers can be modified with the help of copolymerization and physical mixing. Moreover, they can undergo hydrolytic degradation so degradation rate does not varied significantly between host tissues. On the other hand, they cannot attach the cells without some significant biomolecules. Therefore, their surface is modified with the biomolecules to induce cell attachment, proliferation, migration, and differentiation. Synthetic polymers have an important disadvantage that they can form undesired products (i.e., acids) during degradation. Increasing acidity in the native tissue can affect the homeostasis and create immunological responses such as inflammation and fibrous encapsulation [90]. The most common synthetic polymers are polyesters and the others are polyanhydrides, polycarbonates, and polyphosphazenes [91].

2.4.3.4. Poly (propylene fumarate)

PPF consists of repeating unit including one unsaturated C-C double bond and two ester groups [88]. It is linear polyester which degrades by simple hydrolysis of ester bonds into nontoxic compounds. These nontoxic compounds are fumaric acid and propylene glycol. Its degradation duration depends on polymer characteristics. Generally, molecular weight, cross-linker type, and cross-linking density are the most affecting polymer characteristics [92]. The unsaturated double bond allows chemical, photo, or thermal-initiated cross-linking of PPF. Furthermore, this double bond provides cross-linking via free radical polymerization by itself or with a variety of crosslinking agents such as methyl methacrylate (MMA), N-vinyl pyrrolidinone (NVP), and biodegradable macromers of PPF-diacrylate or poly(ethyleneglycol)-diacrylate. The chemical structure of the PPF is presented in Figure 2.5.

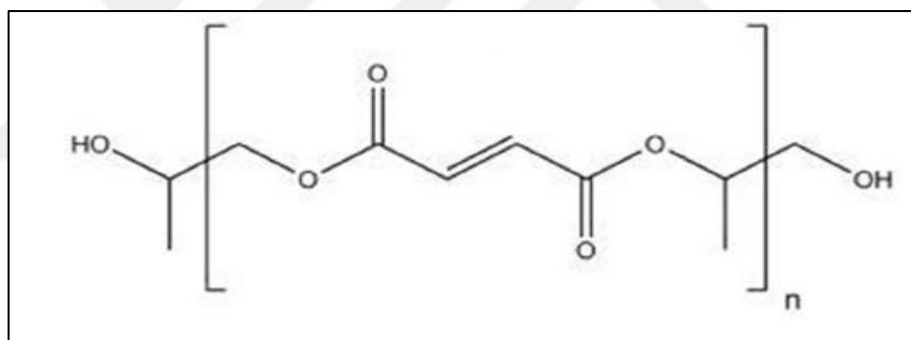


Figure 2.5. Chemical structure of PPF [93]

Also, radical polymerization can be achieved with photoinitiation in the presence of photoinitiators like bisacylphosphine oxide (BAPO) [94]. As a result, cured PPF can enhance compressive and tensile strength and is generally used as biomedical applications (i.e. orthopaedic implants, scaffolds, controlled bioactive factor delivery systems, and cell transplantation vehicles) because of its good mechanical strength, biocompatibility, osteoconductivity, injectability, and handling characteristics [88, 89, 95]. Molecular weight of the PPF varies between 500 Da to 4,000 Da and polydispersities are less than 1.4 [96]. The molecular characteristics and polydispersity of PPF influence mechanical properties and degradation kinetics of crosslinked PPF networks [97]. For example, if molecular weight of the PPF increases, the viscosity also increases and it can affect the handling

characteristics of the desired polymer. Therefore, PPF-based synthetic polymers can be produced by taking into a wide range of parameters into consideration for the applications.

There are a number of synthetic routes for PPF. Trimer intermediate is produced in most of the routes and it is polymerized with step-growth polymerization. A bone putty including PPF was patented firstly in 1988. In this patent, PPF was synthesized by using a p-toluene sulfonic acid-catalyzed transesterification of diethyl fumarate and propylene glycol [98]. After that in 1989, PPF was synthesized by a condensation reaction of fumaric acid with propylene glycol by Gerhart and Hayes [98]. Moreover, again 1989, two trimers (bis-propylene glycol fumarate and 1,2-propylene glycol dibutenoate) were prepared and polymerized to form PPF. As it can clearly be seen that PPF can be synthesized in different routes. PPF synthesis methods are divided into two groups with respect to the number of steps of the synthesis: one-step method and multistep method. However, in more recent methods, PPF has been synthesized in two-step process. The first step includes reaction of diethyl fumarate and propylene glycol in an inert atmosphere and the second step includes transesterification of the bis(hydroxypropyl) fumarate intermediate to produce PPF.

While PPF has hydrophobic surface properties that negatively impacts on cell attachment, copolymerization with hydrophilic polymers (i.e. polyethylene glycol-PEG) or modification with peptides are commonly used methods for increasing PPF hydrophilicity [99]. It was revealed that copolymerized PPF with PEG supported endothelial cell attachment and proliferation [100]. PPF can be combined with ceramic particles (i.e. calcium phosphate, calcium carbonate) for the purpose of cancellous bone replacement applications [101]. Also, copolymers of PPF with polycaprolactone have been used as an injectable scaffolds for the healing of bone defects [102]. Unsaturated PPF and cross-linked PPF microparticles are used for the development of bone cements in the purpose of craniofacial bone repair applications [103]. Besides, thermoreversible block copolymers of PPF and methoxypoly(ethylene glycol) are used as a drug delivery systems [104]. Porous PPF scaffolds are used in different applications such as magnetic resonance imaging-directed implantation, drug-dispensing materials and/or drug carriers for tumor treatment. On the other hand, composites of cross-linked PPF have great mechanical properties. For instance, PPF- beta-tricalcium phosphate (β -TCP) composites have approximately 1,200 MPa modulus strength and 300 MPa yield strength similarly with the trabecular bone [105]. Mechanical properties of the PPF are also improved by using cross-linking agents

such as propylene fumarate diacrylate and poly(ethylene glycol)-dimethacrylate. Fisher *et al.* indicated the *in vivo* osteoconductivity of the PPF scaffolds by using rabbit incisor extraction socket model [106]. However, PPF alone did not show osteoinductivity, it had to be modified by using osteoinductive factors.

TGF- β 1-coated PPF was used to improve osteoinductivity of PPF scaffold [107]. In addition, cell attachment, proliferation, and growth of mouse preosteoblast cells were enhanced when hydroxyapatite (HA) nanoparticles were added to PPF scaffold [108]. PPF can also be incorporated with other polymers. For instance, polyethylene glycol is used to enhance endothelial cell attachment and proliferation [93]. All of these studies demonstrated that PPF based scaffolds have a crucial potential to promote bone regeneration.

2.4.3.5. Polyvinyl phosphonic acid (PVPA) and derivatives

Phosphonated polymers have been used in many different applications such as antimicrobial coatings, dental materials, thermoresponsive materials, and proton-exchange membranes. These negatively-charged polymers can bind to variety of inorganic surfaces and metal ions with hydrogen bonding. PVPA is a water soluble polymer and includes a very high concentration of phosphonic acid units which bind to the polymer backbone [109]. PVPA indicates a strong polyelectrolyte effect providing the preparation of potential bone tissue scaffolds. PVPA can able to mimic phosphorylated non-collagenous proteins (i.e. bone sialoprotein) which have a function in mineralization of a bone matrix. A number of studies indicated that PVPA can act as templating mechanism to mediate matrix mineralization [79, 101, 110]. Therefore, this osteoconductive and osteoinductive polymer has been used as a scaffold to enhance bone regeneration.

In the development of PVPA based scaffolds, the number of phosphonic groups and different monomers can have different effects on resulting polymer such as hydrophilicity, swelling capacity, biocompatibility, and mechanical properties. Greish and Brown have developed a novel biopolymer which contains HA and calcium poly(vinylphosphonate) salt. This biomaterial indicated good mechanical properties due to the functionality of phosphonic groups [111, 112]. In another *in vitro* cell culture study, osteogenic cell adhesion, differentiation, and mineralization were enhanced with PVPA-modified surfaces

[113]. Furthermore, different concentrations of PVPA were grafted onto acrylamide surfaces of prepared biomaterial. It was indicated that pre-osteoblast cells have attached and proliferated successfully on the surfaces of this biomaterial [113]. Therefore, the results of all of these studies emphasize the potential usage of PVPA and its derivatives in BTE applications.

2.5. AIM OF THE STUDY

Bone tissue is a unique part of the human physiology that has many functions such as support of many organs and tissues, mechanical protection, movement, storage of minerals and multiple progenitor cells, production of blood cells, and regulation of blood pH. It has a capacity to regenerate after injury, trauma, or disease through the processes of bone healing. However, bone tissue healing is limited in the critical size defects and has to be supported with tissue engineering constructs. The use of synthetic polymers has become widespread in the field of tissue engineering. However, the most widely used synthetic polymers (i.e. PLGA, PCL, PGA) are generally fragile and have not functional diversity in the backbone. Therefore, these properties lead to limit their usage in BTE applications. In recent years, PPF have attracted a lot of interest in BTE applications because of their superior biocompatibility, biodegradability, and mechanical property. The need for novel PPF based scaffolds and reproducible design techniques have the greatest importance in this field. Therefore, in our study, PPF and vinyl phosphonic acid (VPA) or vinyl phosphonic acid diethyl ester (VPES) based biodegradable and biocompatible polymer systems were developed to be used as scaffolds for BTE applications. It was expected that the use of VPA and VPES in the cross-linking of PPF increases the biocompatibility and the introduction of the phosphonic acid, ester structures, and β -TCP to the network also supports bone tissue formation by increasing the osteoblast activity and decreasing the osteoclast activity. Therefore, the main purpose of this study was to determine the role of PPF/VPA and PPF/VPES based novel scaffolds in bone regeneration and the secondary aims were as follows:

- Investigate the effect of UV cured PPF/VPA and PPF/VPES scaffolds (in the presence of different BAPO concentrations) on human osteoblast (HOb) cell biocompatibility, cell attachment, mineralization, ALP activity, and OC activity.

- Investigate the effects of BT cured PPF/VPES and PPF/VPES- β -TCP based scaffolds and the effects of different β -TCP concentrations on HOb cell biocompatibility, cell attachment, mineralization, ALP activity, and OC activity.



3. MATERIALS AND METHODS

3.1. MATERIALS

TrypLE™ express dissociation reagent 1X w/o phenol red sterile, penStrep penicillin streptomycin sterile, heat inactivated fetal bovine serum sterile (EU approved origin), Dulbecco's modified eagle medium 1g/L D-glucose, with pyruvate, w/o L-glutamine w/o phenol red (sterile) were purchased from Gibco® by life technologies™. Silver nitrate solution (5 per cent), sodium thiosulfate solution (5 per cent), nuclear fast red solution were purchased from Diagnostic BioSystems. Dexamethasone (97 per cent), β -glycerophosphate disodium salt hydrate BioUltra, suitable for cell culture (≥ 99 per cent), and L-ascorbic acid 2-phosphate sesquimagnesium salt hydrate (≥ 95 per cent) were purchased from SIGMA life science and Dulbecco's phosphate buffered saline (w/o calcium, w/o magnesium, 10X, sterile) was purchased from SAFC Biosciences™. Cell culture flasks (T25, T75, T150) and 24-48-96 well plates were purchased from TPP® Techno Plastic Products AG, Switzerland. Furthermore, serological pipettes (5 ml, 10 ml, 25 ml), falcon tubes (15 ml, 50 ml), and micropipettes were purchased from Jet Biofil®, China, IsoLab, Germany, Eppendorf Research, Germany, respectively.

3.2. METHODS

3.2.1. Preparation of PPF Based Scaffolds

Both low and high molecular weight PPF polymers were synthesized and prepared by PhD student, Görkem Cemali and following methods were used. Synthesized low molecular weight PPF ($M_n=1190$ g/mol, $M_w=1678$ g/mol) was cured in the presence of two phosphonic acid based co-monomers, VPA and VPES, at 70/30 ratio in the presence of 2 per cent and 3 per cent BAPO as a photoinitiator. Prepared PPF/VPA (70/30) and PPF/VPES (70/30) were exposed UV light ($\lambda=260$ nm) for 2 hours. Then, samples were cut into equal pieces, sterilized under UV light, and used as a scaffold for *in vitro* cell culture studies.

On the other hand, synthesized high molecular weight PPF ($M_n=2558$ g/mol, $M_w=4768$ g/mol) was cured with VPES co-monomer and β -TCP was added to homogenized PPF/VPES mixture (70/30) at different ratios (5 per cent, 10 per cent, 15 per cent, and 20 per cent) in the presence of 3 per cent BP and 0.3 per cent N,N'-dimethyltoluene (DMT). Homogenized mixture was placed in preheated vacuum oven at 37 °C for 2 hours. Prepared PPF/VPES- β -TCP samples were cut into equal pieces, sterilized under UV light, and used as a scaffold for *in vitro* cell culture studies. PPF/VPES- β -TCP based composites were prepared by MSc student, Avram Aruh.

3.2.2. Osteoblast Cell Culture

Human osteoblast cells (HOb) (The European Collection of Cell Cultures, UK) (Cell line no. 406-05a) were cultured in Dulbecco's modified Eagles medium (DMEM) supplemented with 10 per cent FBS, antibiotics (1 per cent of penicillin, streptomisin, and amphotericin) and 50 μ M ascorbic acid. HOb cells were cultured under standard conditions at 37°C with 90 per cent humidity and 5 per cent CO₂ in incubator (Thermo Scientific, USA). Culture medium was replenished every 2 days. When the desired number of cells was reached, these cells were removed from cell culture flasks using TrypLE Express Dissociation Reagent (1X) w/o phenol red and centrifuged at 2,000 rpm for 5 minutes. The HOb cells were counted with hemocytometer and used in further experiments.

3.2.3. *In vitro* Cell-Biomaterial Interaction Studies

Sterilized samples were placed in cell culture plates and HOb cells were seeded onto each scaffold at a density of 5×10^3 cells/well. Cells were cultured with osteogenic medium consisting of DMEM supplemented with 10 per cent FBS, antibiotics (1 per cent of penicillin, streptomisin, and amphotericin), 50 μ M ascorbic acid, 100 nM dexamethasone, 50 μ M ascorbic acid and 10 mM β -glycerophosphate under standard conditions at 37°C with 90 per cent humidity and 5 per cent CO₂ for different incubation times.

3.2.3.1. Scanning Electron Microscopy (SEM)

Cell containing scaffolds were incubated for 7, 14, 21, and 28 days in osteogenic media. Culture medium was replenished every three days. After each time points, samples were washed with cacodylate buffer, fixed with 2.5 per cent of glutaraldehyde solution for 1 hour at room temperature and washed with cacodylate buffer again. Dry samples were coated with 10 nm gold and examined by SEM.

3.2.3.2. Cell proliferation-MTS assay

Cell seeded scaffolds were incubated under the standard conditions at 37 °C with 90 per cent humidity and 5 per cent CO₂ for up to 7, 14, and 21 days and supplied with fresh osteogenic medium every 3 days. At the end of time intervals, CellTiter 96[®] AQueous One Solution Cell Proliferation Assay (Promega) was carried out according to manufacturer's instructors. Cell medium was aspirated from each well and each sample was incubated in 500 µl of prepared MTS solution for 2.5 hours (Incubation period was determined according to calibration curve). After that, 100 µl aliquots of the incubation solution were transferred into a 96-well plate (Orange Scientific, Belgium) and absorbance was measured at 490 nm on a ELISA plate reader (Bio-Tek ELx800 Absorbance microplate reader, USA). The number of cells for each sample were calculated according to calibration curve of the HOB cells. Calibration curve was obtained with carrying out MTS assay on known cell numbers (1×10^3 , 2×10^3 , 3×10^3 , 5×10^3 , 7×10^3 , 8×10^3 , 10×10^3 , 20×10^3 cells).

3.2.3.3. von Kossa Staining

After 3 days of incubation, cell seeded scaffolds were divided into two groups and while the first group was cultured in osteogenic medium, the other one was cultured in standard cell culture medium (DMEM w/o phenol red). Both groups were incubated under standard conditions at 37 °C with 90 per cent humidity and 5 per cent CO₂ for up to 7, 14, 21, and 28 days and supplied with fresh osteogenic medium or cell culture medium (DMEM w/o phenol red) every 3 days. At the end of the specific time intervals, culture medium was aspirated from all samples and 5 per cent of silver nitrate solution was added. Samples

were incubated for 60 minutes under the UV light. Thereafter, samples were washed three times with dH₂O and 5 per cent of sodium thiosulfate solution was added on samples. After 3 minutes incubation time, samples were washed with tap water. Nuclear fast red solution was added on samples and incubated for 5 minutes. Samples were washed with absolute ethanol for three times and dehydrated samples were evaluated. This experiment was conducted in duplicate.

3.2.3.4. Alkaline Phosphatase

Cell containing scaffolds were cultured with osteogenic medium under standard conditions at 37°C with 90 per cent humidity and 5 per cent of CO₂ for up to 4, 7, 14, 21, and 28 days. At the time of specific time intervals, culture medium was aspirated from all samples and 200 µl of physiological saline was added into each well for washing. Cell lysis was achieved by using 50 µl of extraction solution. Then, 50 µl of substrate solution (*p*-nitrophenyl phosphate solution) was added into each well and incubated at 37 °C for 1 hour. After incubation period, 50 µl of stop solution (0.9 N NaOH) was added into each cell. The absorbance was measured at 405 nm after color formation. ALP activities of attached cells were measured according to TRACP and ALP assay kit (TaKaRa). ALP assay were conducted in duplicate.

3.2.3.5. Osteocalcin Assay

Medium of the cell containing scaffolds was replenished every three days. At the end of 7, 14, 21, and 28 days of incubation, 25 µl of media was collected from the samples and transferred to into 8-well strips. These strips were divided into 3 groups: standard, control, and sample. Also, 25 µl of standard and control, and then 100 µl of Anti-OST-HRP conjugate were added into appropriate wells. Plates were covered and incubated for 2 hours at room temperature. After incubation period, solutions were aspirated from all wells and they were washed with wash solution for 3 times. Following the washing step, 100 µl of chromogen solution was added into each well and plates were incubated for 30 minutes at room temperature in the dark. After adding 100 µl of stop solution, color was changed from blue to yellow. The absorbance was measured at 405 nm on a ELISA plate reader

(Bio-Tek ELx800 Absorbance microplate reader, USA). Osteocalcin was quantified using human osteocalcin (hOST) ELISA kit (Invitrogen, UK).

3.2.4. Statistical Analysis

The values were expressed as mean \pm standard deviation (mean \pm SD). To determine the statistical significance of the results Student's t-test was performed. Significance was assigned at p values less than 0.05.



4. RESULTS

In the first part of scaffold preparation, UV-cured PPF/VPES and PPF/VPA samples that were synthesized with different photoinitiator (BAPO) concentrations were investigated. First, PPF/VPA with 2 per cent and 3 per cent BAPO were prepared. PPF/VPA with 1 per cent BAPO was also tried but there was no cure with this BAPO concentration. In the same way, PPF/VPES with 1 per cent and 2 per cent BAPO were prepared. Since these BAPO concentrations were enough for cure, 3 per cent BAPO concentration was not being tried. Figure 4.1 indicates the UV-cured PPF/VPES samples with 1 per cent and 2 per cent BAPO. It was observed that these samples were successfully cured with two different BAPO concentrations and hardened under UV light. Figure 4.2 indicates the UV-cured PPF/VPA samples with 2 per cent and 3 per cent BAPO. It was observed that PPF/VPA (70/30) sample including 3 per cent BAPO were better cured than sample including 2 per cent BAPO which was partially cured. Additionally, UV-cured polymers containing VPES were better cured than VPA containing polymers.

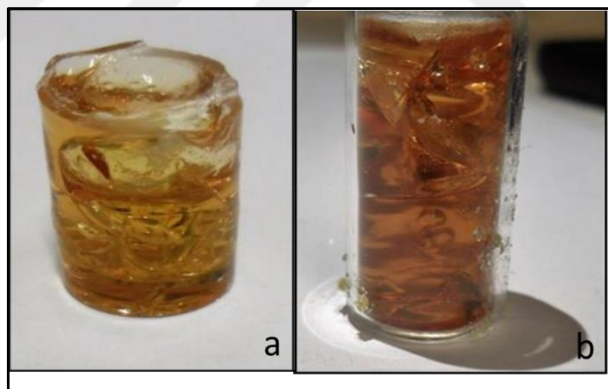


Figure 4. 1. UV-cured PPF/VPES (70/30) polymers in the presence of a) 1 per cent BAPO
b) 2 per cent BAPO

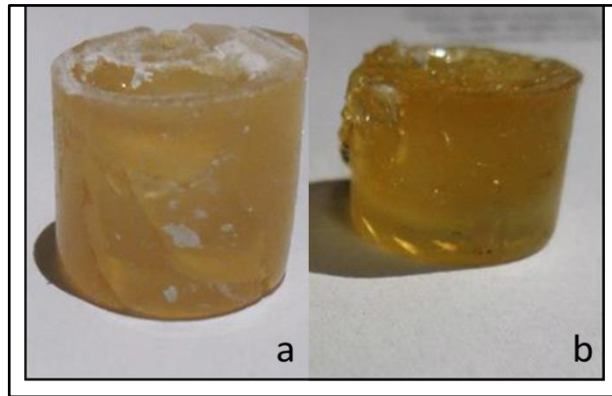


Figure 4.2. UV-cured PPF/VPA (70/30) polymers in the presence of a) 2 per cent BAPO b) 3 per cent BAPO

In the second part of scaffold preparation, BT-cured PPF/VPES samples were prepared and characterized. In here, preparation of BT-cured PPF/VPA (70/30) scaffold was also tried but the scaffolds could not get cured successfully. Therefore, only PPF/VPES (70/30) samples were used for this part (Figure 4.3.a).

In the third part scaffold preparation, BT-cured PPF/VPES samples including different ratios of β -TCP were prepared and characterized. Figure 4.3.b-e represents BT-cured PPF/VPES (70/30) samples including different ratios of β -TCP. It was observed that all samples cured successfully. Also, the usage of N,N'-DMT as a catalyst gave a brown color to the samples.

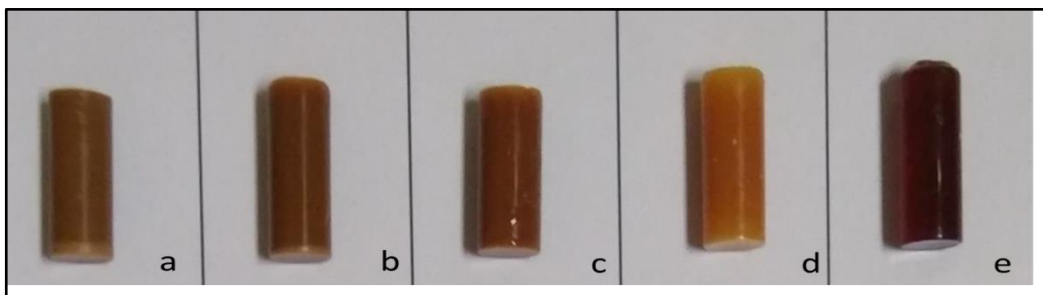


Figure 4.3. BT-cured PPF/VPES polymers a) without β -TCP b) 5 per cent β -TCP c) 10 per cent β -TCP d) 15 per cent β -TCP e) 20 per cent β -TCP in the presence of 3 per cent BP and 0.3 per cent N,N'-DMT

All these scaffolds were characterized using contact angle goniometer, dynamic mechanical analyzer, thermogravimetric analyzer, scanning electron microscopy, and

Fourier-transform infrared spectroscopy by Görkem Cemali and Avram Aruh. Also, biodegradation studies were conducted.

4.1. *IN-VITRO* CELL-BIOMATERIAL INTERACTION

4.1.1. Scanning Electron Microscopy (SEM) Analysis

SEM images of cell-seeded scaffold surfaces on day 7, 14, 21, and 28 are given in Figure 4.4-4.7.

The morphology, attachment, spreading, and proliferation characteristics of HOb cells on UV-cured (Figure 4.4 and 4.5) and BT-cured scaffolds (Figure 4.6 and 4.7) were visualized using SEM analysis. It was observed that HOb cells were able to attach and spread on all sample types. SEM images indicate that HOb cells had the normal osteoblastic morphology. Also, the results show that the cells adhered and proliferated in rough surfaces and cellular interactions were provided for all sample types.

It was visualized that HOb cells penetrated inside the UV-cured PPF/VPA scaffold samples (Figure 4.4). In both type of UV-cured PPF/VPA samples, HOb cells spread and proliferated onto the scaffold side by side. While the number of adhered and proliferated HOb cells increased throughout 28 days of incubation for both UV-cured PPF/VPA samples (Figure 4.4 a-d, e-h), extensive cell spreading was observed in UV-cured PPF/VPA sample including 3 per cent BAPO.

Similarly in UV-cured PPF/VPES samples, the adhered and proliferated HOb cells increased with increasing incubation time. These differences were clearly visualized when the results of 7 days of incubation (Figure 4.5.a, e) and 28 days of incubation (Figure 4.5.d, h) compared to each other. The osteoblastic morphology of the HOb cells was obviously seen in Figure 4.5.c. Cell sheets were observed on the surfaces of the all UV-cured PPF/VPES samples and the most of the HOb cells formed bridging orthogonal filopodia and ECM (Figure 4.5). Extensive cell attachment and cell spreading were observed in UV-cured PPF/VPES (70/30) samples including 1 per cent BAPO (Figure 4.5. a-d). Additionally, it was observed that HOb cells spread onto the scaffolds side by side including 1 per cent BAPO (Figure 4.5.a).

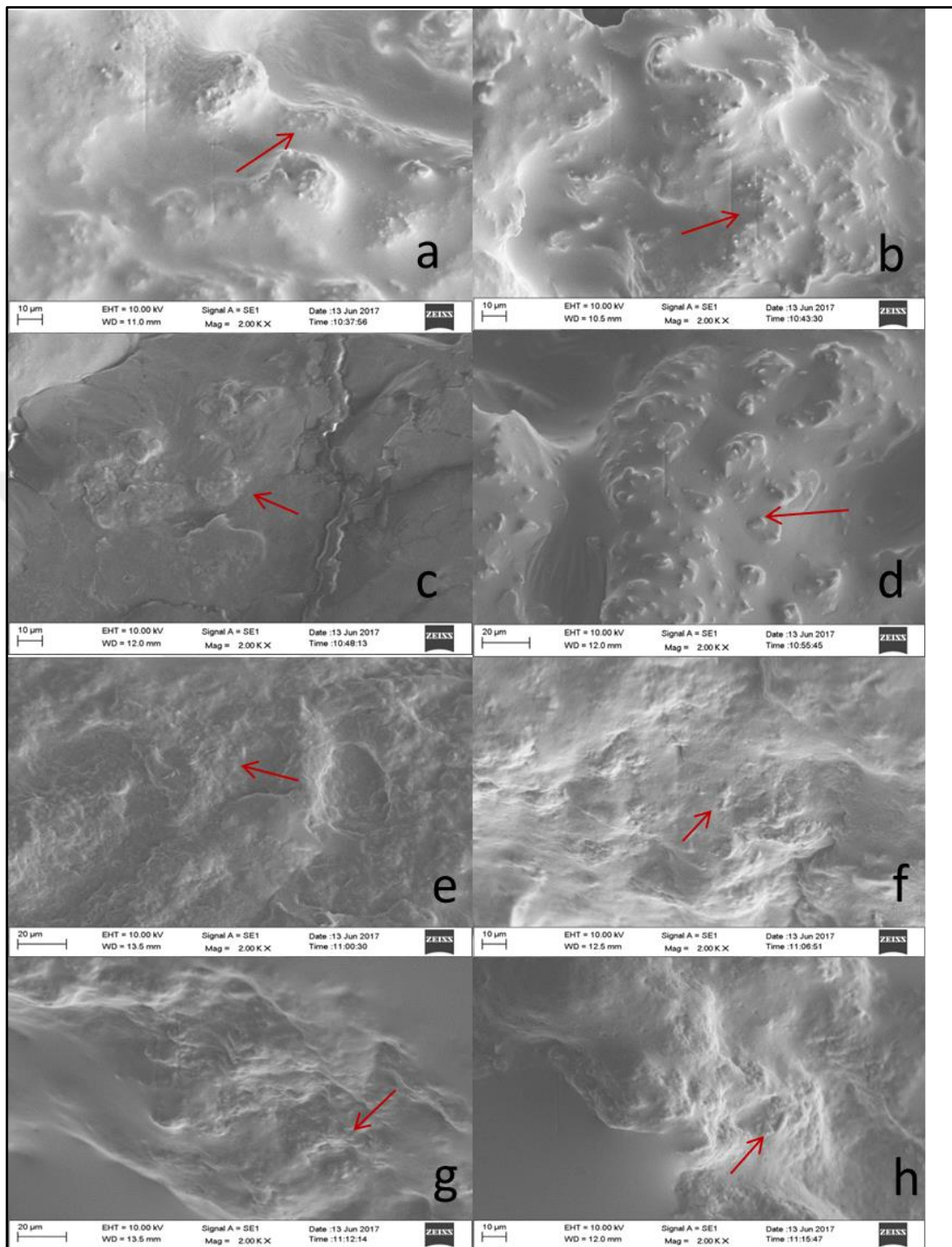


Figure 4.4. SEM images of UV-cured PPF/VPA (70/30) samples in the presence of (a-d) 2 per cent BAPO, (e-h) 3 per cent BAPO after (a, e) 7, (b, f) 14, (c, g) 21, and (d, h) 28 days of incubation. Magnification: 2,000 X. Arrows show HO_b cells.

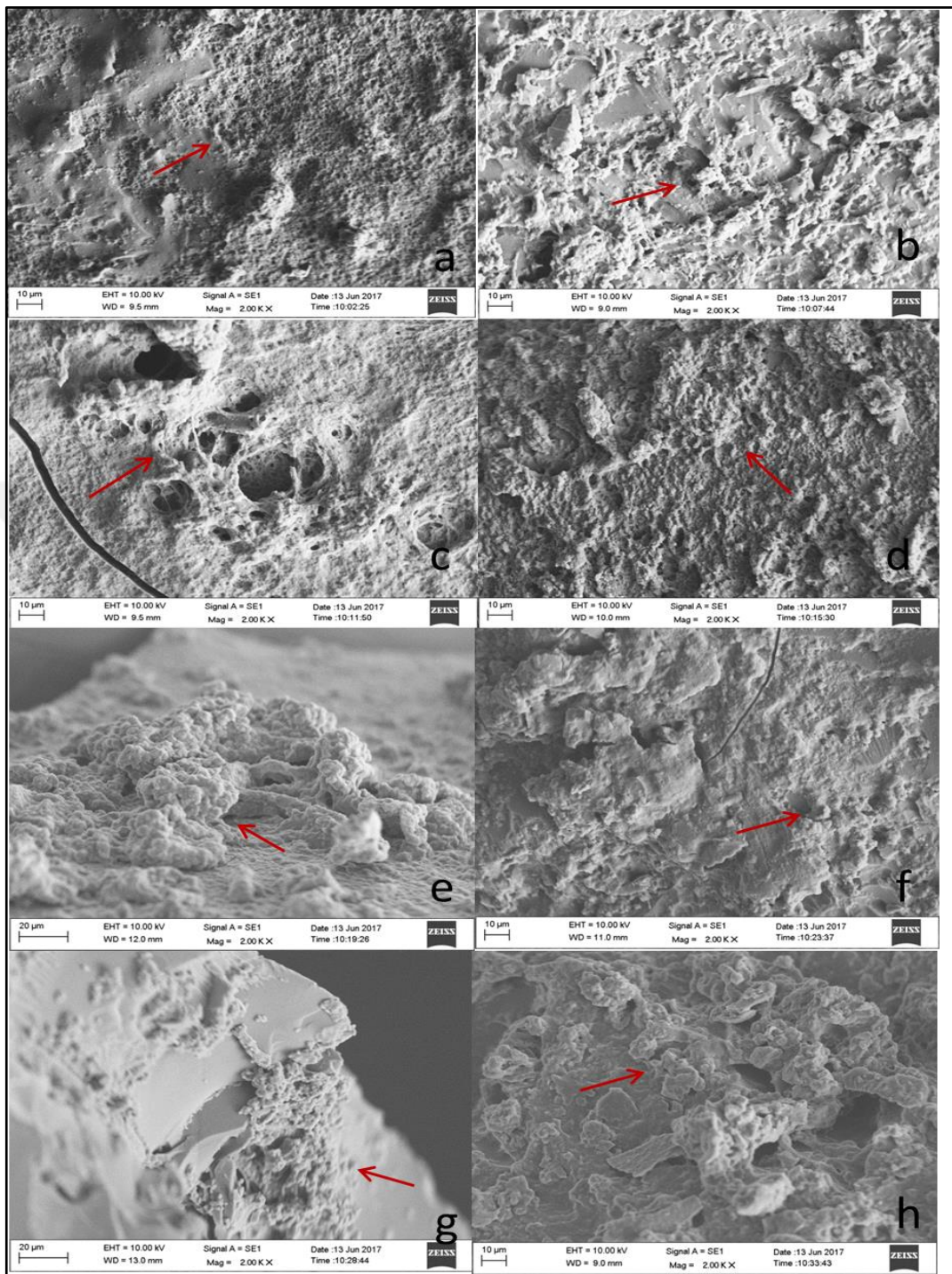


Figure 4.5. SEM images of UV-cured PPF/VPES (70/30) samples in the presence of (a-d) 1 per cent BAPO, (e-h) 2 per cent BAPO after (a, e) 7, (b, f) 14, (c, g) 21, and (d, h) 28 days of incubation. Magnification: 2,000 X. Arrows show HOB cells.

Extensive cell attachment and cell spreading was observed and the greater number of cells adhered and proliferated on all types of BT-cured scaffolds (Figure 4.6 and 4.7). The osteoblastic morphology was visualized on all types of BT-cured scaffolds. As it was seen in Figure 4.6 and 4.7, HOB cells preferred the rough surfaces for attachment and proliferation. Similarly in UV-cured samples, the adhered and proliferated HOB cells on BT-cured PPF/VPES samples increased with increasing incubation time. These differences were clearly observed when the results of 7 days of incubation (Figure 4.6.a) and 28 days of incubation (Figure 4.6.d) compared to each other. Also, HOB cells spread and proliferated onto the BT-cured PPF/VPES scaffold side by side after 21 days of incubation (Figure 4.6.d).

Moreover, HOB cells spread and proliferated well on composites of BT-cured PPF/VPES samples (Figure 4.7). Extensive cell sheets were visualized on the surfaces of all BT-cured composites. The surface of the cell seeded scaffolds were covered by newly formed ECM. Newly formed ECM formation was obviously visualized in composites including 10 per cent β -TCP after 14 days of incubation (Figure 4.7.f). Similarly in other samples, HOB cells adherence, spreading, and proliferation increased throughout 28 days of incubation (Figure 4.7.a-d, e-h, i-l, m-p).

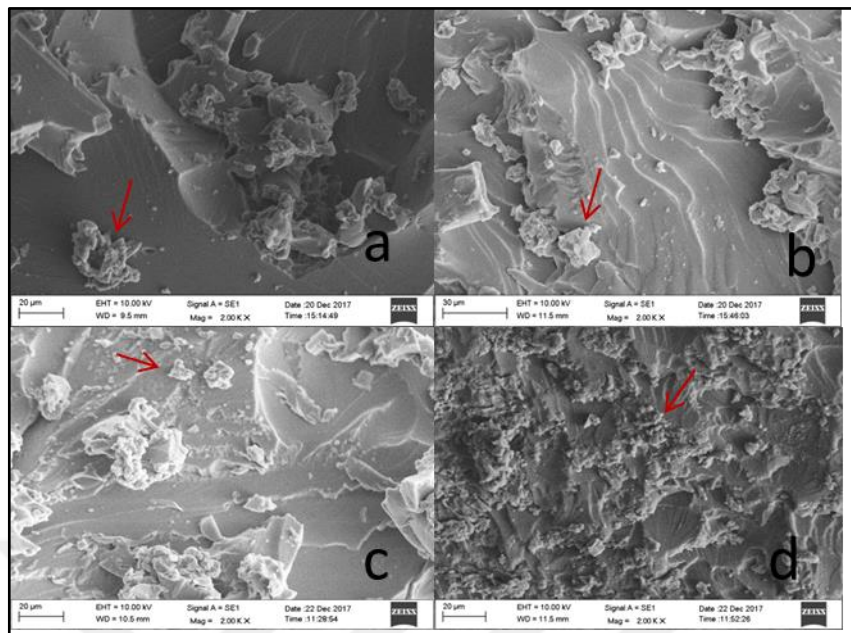


Figure 4.6. SEM images of BT-cured PPF/VPES (70/30) samples in the presence of 3 per cent BP and 0.3 per cent N,N'-DMT on a) day 7 b) day 14 c) day 21 d) day 28.

Magnification: 2,000 X. Arrows show HOB cells.

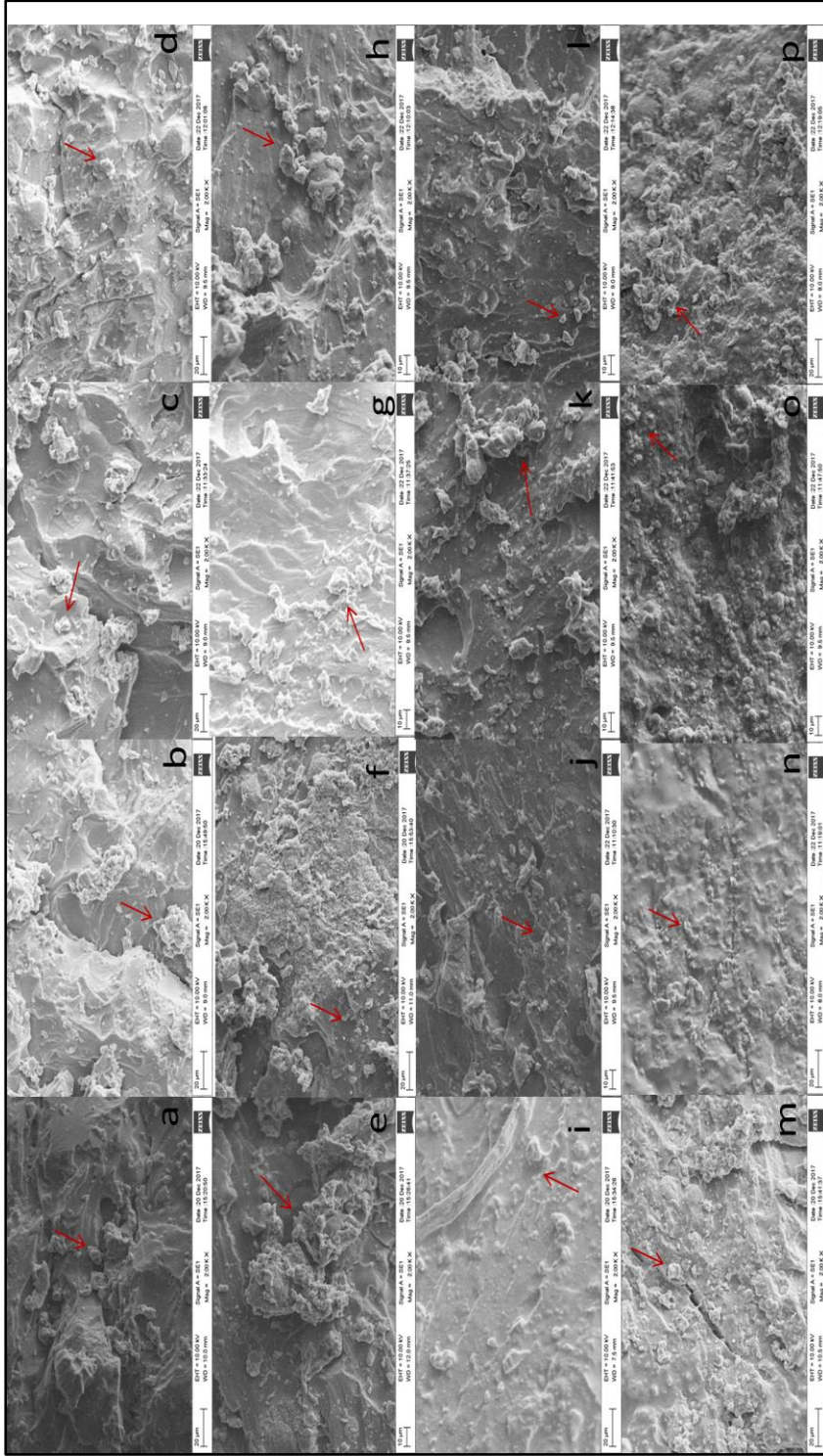


Figure 4.7. SEM images of BT-cured PPF/VPES (70/30) composites including (a-d) 5 per cent, (e-h) 10 per cent (i-l) 15 per cent, and (m, p) 20 per cent β -TCP in the presence of 3 per cent BP and 0.3 per cent N,N' -DMT after (a, e, i, m) 7, (b, f, j, n) 14, (c, g, k, o) 21 and (d, h, l, p) 28 days of incubation. Magnification: 2,000 X. Arrows show HO cells

4.1.2. Cell proliferation-MTS assay

Proliferation and attachment of HOb cells on crosslinked PPF samples were investigated using MTS assay on days 7, 14, 21, and 28 (Figures 4.8 and 4.9).

The number of viable HOb cells increased significantly between day 7 and 28 in only cell containing group (control group) ($p < 0.01$). A significant increase was also observed in the cell number of control group between day 7 and 14, day 21 and 28 ($p < 0.01$) (Figure 4.8).

Viable HOb cell number in PPF/VPA samples were higher than the ones in both PPF/VPES and only HOb cell groups in all time points (Figure 4.8). Although, the viable cell number increased with increasing incubation time, a significant increase was only observed between day 7 and day 28 for PPF/VPA sample with 3 per cent BAPO ($p < 0.01$).

The viable HOb cell number decreased between day 7 and day 14, but this decrease was not significant for PPF/VPA samples with 2 per cent BAPO. After 14 days of incubation, the number of viable HOb cells increased significantly ($p < 0.01$). Also, there was a significant increase between day 21 and day 28 for PPF/VPA samples with 2 per cent BAPO ($p < 0.01$).

When we compare the effect of BAPO concentration on HOb cell proliferation for VPA samples, a significant difference was observed only on day 14 between samples cured in the presence of 2 per cent BAPO and 3 per cent BAPO ($p < 0.05$). Both, PPF/VPA samples with two different BAPO concentrations supported cell proliferation with a similar pattern. In both samples, cell proliferation increased throughout 28 days of incubation. Initial cell attachment was the same on both samples.

In other respects, BAPO concentration had a significant effect on PPF/VPES samples on day 21 and 28 ($p < 0.01$). With respect to initial cell attachment, there was no difference between two PPF/VPES samples with two different BAPO concentrations. UV-cured PPF/VPES (70/30) sample including 2 per cent BAPO supported cell proliferation more than the one including 1 per cent BAPO. A significant difference was observed in the cell number of VPES samples with 2 per cent BAPO on each time points except the one between day 7 and 14 ($p < 0.01$). However, there was a significant decrease in 1 per cent

BAPO including samples between day 7 and 28 ($p < 0.05$), day 14 and 21 ($p < 0.01$), day 21 and 28 ($p < 0.05$).

When we compare the cell proliferation on VPES and VPA scaffolds, it can be seen that PPF/VPA scaffolds supported cell proliferation better than the PPF/VPES scaffolds.

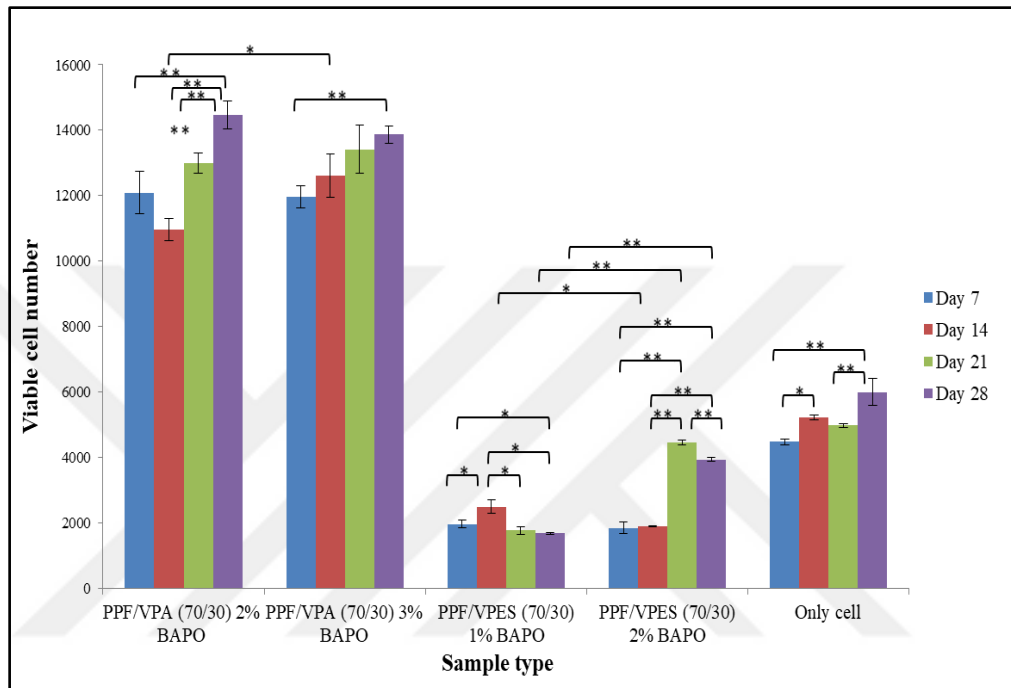


Figure 4.8. Proliferation of HOB cells on UV-cured PPF/VPA (70/30) and PPF/VPES (70/30) samples with different BAPO concentrations. Initial cell seeding density was 5×10^3 cells/sample. * and ** indicate a significant difference with a $p < 0.05$ and $p < 0.01$, respectively.

In this part, cell proliferation and initial cell attachment were also investigated on BT-cured PPF/VPES scaffolds with and without β -TCP.

When HOB cells cultured alone, cells proliferated more compared to the cells seeded on BT-cured samples (Figure 4.9). After 21 days of incubation, cell proliferation decreased in only cell containing group (control group). Similarly, this decrease was also recorded for all BT-cured samples. A significant increase was observed in the cell number of all BT-cured samples between day 7 and day 21 ($p < 0.01$). There was a significant difference between all incubation time points in terms of cell number for samples with 0 per cent, 10

per cent and 20 per cent β -TCP except the one between day 7 and day 14. All BT-cured PPF/VPES samples indicated a peak on day 21 in terms of cell proliferation and the highest viable HOb cell number was recorded on PPF/VPES sample with 20 per cent β -TCP. Also, on day 28 the highest viable cell number was recorded for the samples with 5 per cent β -TCP. However, it was observed that different β -TCP ratios at each time points did not have a significant effect on cell proliferation. All BT-cured samples supported the proliferation throughout 28 days of incubation. Therefore, no difference was observed when we compared BT-cured PPF/VPES samples and its composites with respect to initial cell attachment and proliferation. All BT-cured samples had a similar proliferation pattern throughout 28 days of incubation.

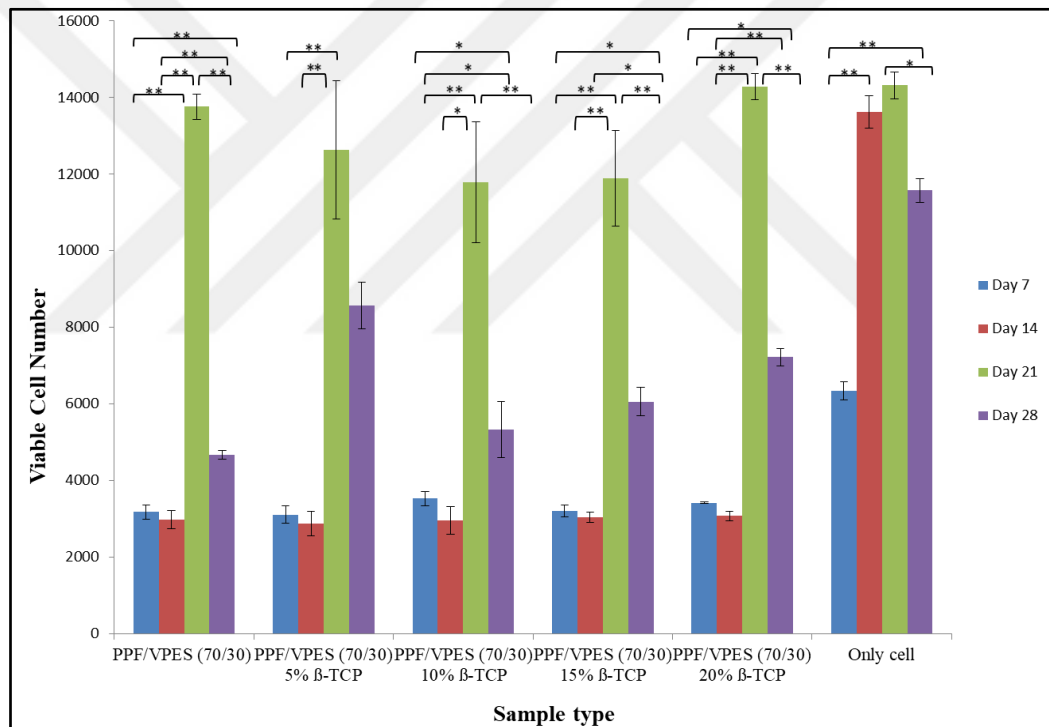


Figure 4.9. Proliferation of HOb cells on BT-cured PPF/VPES (70/30) samples and its composites with different β -TCP ratios. Initial cell seeding density was 5×10^3 cells/sample.

* and ** indicate a significant difference with a $p < 0.05$ and $p < 0.01$, respectively.

4.1.3. von Kossa Staining

Mineralization on the samples was determined by von Kossa staining throughout 28 days of incubation (Figure 4.10 and Figure 4.11). A positive staining of mineralized regions was observed in all UV-cured PPF/VPA (70/30) samples after 7 days of incubation (Figure 4.10.a, b). After 14 days of incubation, these samples indicated largely mineralized regions with dark color. There was no significant difference between UV-cured PPF/VPA (70/30) samples containing 2 per cent and 3 per cent BAPO and both of them supported osteogenesis in the same way. A positive staining was observed after 14 days of incubation for UV-cured PPF/VPES (70/30) samples containing 1 per cent BAPO (Figure 4.10.c, d). Only, the UV-cured PPF/VPES (70/30) sample containing 2 per cent BAPO showed no sign of mineralization throughout the 21 days of incubations. There was a light pink and red colors on days 7, 14, and 21 and these colors indicate the staining of nucleus, and cytoplasm of HOB cells, respectively. Therefore, sample containing 1 per cent BAPO was more likely to support osteogenesis. In addition, when we compared UV-cured samples in terms of co-monomer types, VPA containing samples had markedly larger mineralized regions and so more likely to support osteogenesis than VPES containing samples.

The qualitative observations of the von Kossa results were verified with using the ColorPic software (Iconico Inc). The hue, saturation, and value of the red, green, and blue colors were described by this program. Hue is the dominant wavelength of light which comprises from blue, red, and green color. Hue is measured in degrees from 0° to 359°. Saturation determines the purity of the color. Lastly, value refers the lightness or darkness of the color. If the value of a color is low, it means that the color is dark and therefore is more mineralization. According to this information, UV-cured PPF/VPA sample with 2 per cent BAPO had the darkest color on day 28 (value=36). Mineralization of the HOB cells on UV-cured samples was ranked as $d < c < b < a$ (Table 4.1).

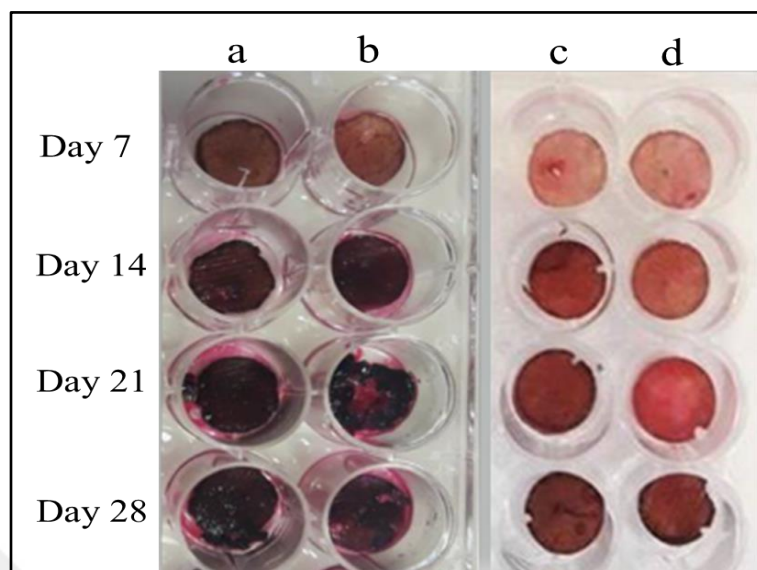


















Figure 4.10. von Kossa staining of UV-cured PPF/VPA (70/30) polymers in the presence of a) 2 per cent BAPO b) 3 per cent BAPO and PPF/VPES (70/30) polymers in the presence of c) 1 per cent BAPO d) 2 per cent BAPO

Table 4.1. von Kossa staining results of UV-cured PPF/VPA and PPF/VPES samples according to ColorPic software

Sample type	Time	Color	Hue	Saturation	Value	Red	Green	Blue
PPF/VPA (70/30) 2% BAPO	Day 7		6	118	82	48	48	44
	Day 14		357	103	57	57	34	35
	Day 21		354	67	38	38	28	29
	Day 28		338	57	36	36	28	31
PPF/VPA (70/30) 3% BAPO	Day 7		149	134	116	116	64	55
	Day 14		341	103	47	47	28	34
	Day 21		311	74	38	38	27	36
	Day 28		328	74	45	45	32	39
PPF/VPES (70/30) 1% BAPO	Day 7		10	126	196	196	115	99
	Day 14		7	173	136	136	54	44
	Day 21		7	171	121	121	49	40
	Day 28		1	146	94	94	41	40
PPF/VPES (70/30) 2% BAPO	Day 7		10	112	198	198	126	111
	Day 14		5	168	172	172	69	59
	Day 21		3	152	198	198	86	80
	Day 28		5	172	110	110	43	36

von Kossa staining of BT-cured PPF/VPES samples with and without β -TCP was also carried out. Figure 4.11 clearly indicates the increasing mineralization of BT cured PPF/VPES- β -TCP samples from day 7 to day 28. A positive staining was also observed in sample without β -TCP. Considering the results obtained with increasing β -TCP ratios, black color intensity increased with increasing β -TCP ratios up to 10 per cent. However, there was not significant difference between samples including 10 per cent, 15 per cent, and 20 per cent β -TCP in terms of black color intensity. Additionally, mineralized regions of BT-cured samples included more intense dark color when compared to UV-cured samples. Accordingly, it can be said that BT-cured samples have more calcium phosphate deposits, and more likely to support ECM formation of HOOb cells.

In other respects, according to ColorPic software the darkest color was recorded for PPF/VPES with 0 per cent and 15 per cent β -TCP throughout 28 days of incubation (Table 4.2). Also, mineralization on PPF/VPES with 0 and 10 per cent β -TCP was close to the one with 15 per cent β -TCP. BT-cured samples had the darkest color compared to UV-cured samples. Therefore, BT-cured samples supported mineralization better than UV-cured samples.

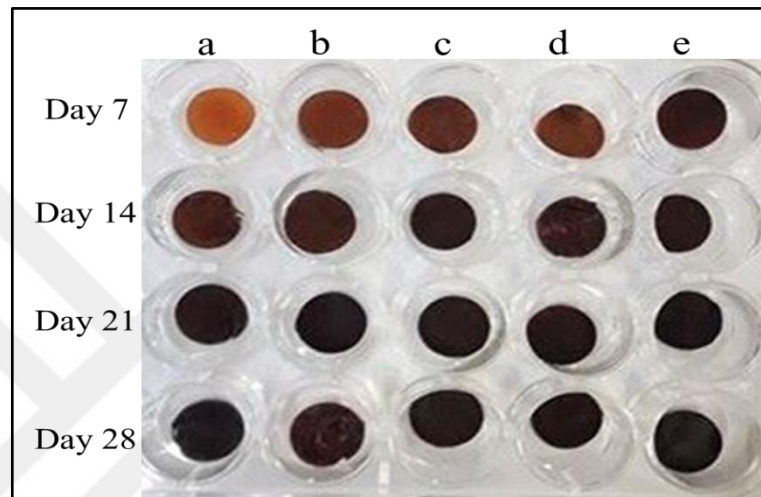


Figure 4.11. von Kossa staining of BT-cured PPF/VPES polymers a) without β -TCP b) 5 per cent β -TCP c) 10 per cent β -TCP d) 15 per cent β -TCP e) 20 per cent β -TCP in the presence of 3 per cent BP and 0.3 per cent N,N'-DMT

Table 4.2. von Kossa staining results of BT-cured PPF/VPES samples and composites according to ColorPic software

Sample type	Time	Color	Hue	Saturation	Value	Red	Green	Blue
PPF/VPES (70/30)	Day 7		16	209	165	165	65	30
	Day 14		8	153	65	65	31	26
	Day 21		348	106	36	36	21	24
	Day 28		340	53	29	29	23	25
PPF/VPES (70/30) 5% β -TCP	Day 7		10	180	106	106	43	31
	Day 14		16	123	56	56	36	29
	Day 21		340	56	41	41	32	35
	Day 28		355	156	36	36	14	16
PPF/VPES (70/30) 10% β -TCP	Day 7		8	139	86	86	45	39
	Day 14		8	89	43	43	30	28
	Day 21		350	76	40	40	28	30
	Day 28		16	85	33	33	25	22
PPF/VPES (70/30) 15% β -TCP	Day 7		18	181	97	97	49	28
	Day 14		354	128	62	62	31	34
	Day 21		354	73	35	35	25	26
	Day 28		18	88	29	29	22	19
PPF/VPES (70/30) 20% β -TCP	Day 7		5	133	48	48	25	23
	Day 14		4	91	45	45	30	29
	Day 21		353	60	38	38	29	30
	Day 28		27	64	36	36	31	27

4.1.4. Alkaline Phosphatase Assay

Alkaline phosphatase expression of the cells on samples throughout 28 days of incubation was determined.

The calibration curve of ALP activity was determined using *p*-nitrophenylphosphate as the substrate. ALP activity of the cells on samples were calculated according to this calibration curve (Appendix A). It was observed that incubation of HObs under osteogenic condition within 28 days resulted in a significant increase in ALP activity for all samples (Figures 4.12 and 4.13). Also, ALP activity increased and decreased cyclically in the HObs cells.

ALP activity of HOB cells decreased significantly between day 7 and day 21 but after 21 days of incubation it increased significantly for UV-cured PPF/VPES sample with 1 per cent BAPO ($p < 0.01$) (Figure 4.12). However, it was observed that ALP activity increased significantly between day 7 and day 14 ($p < 0.05$). UV-cured PPF/VPES sample including 1 per cent BAPO expressed more ALP on day 4 ($p < 0.05$) and day 28 ($p < 0.01$) compared to the one with 2 per cent BAPO. Therefore, VPES sample with 1 per cent BAPO promoted osteogenesis better than the one with 2 per cent BAPO.

Increased ALP activity was observed between day 7 and 14 for VPA sample containing 2 per cent BAPO ($p < 0.01$). Also, ALP activity was observed to peak on day 4 for PPF/VPA sample including 3 per cent BAPO. ALP activity of HOB cells decreased between day 4 and day 14 ($p < 0.01$); day 7 and day 14 ($p < 0.05$). After 28 days of incubation, the highest ALP activity was observed for PPF/VPA sample with 3 per cent BAPO. There was no significant difference between two VPA samples except ALP activity on day 21. These samples almost equally supported osteogenesis.

When we compare the ALP activity on VPES and VPA scaffolds, it can be seen that PPF/VPA scaffolds supported osteogenesis better than the PPF/VPES scaffolds.

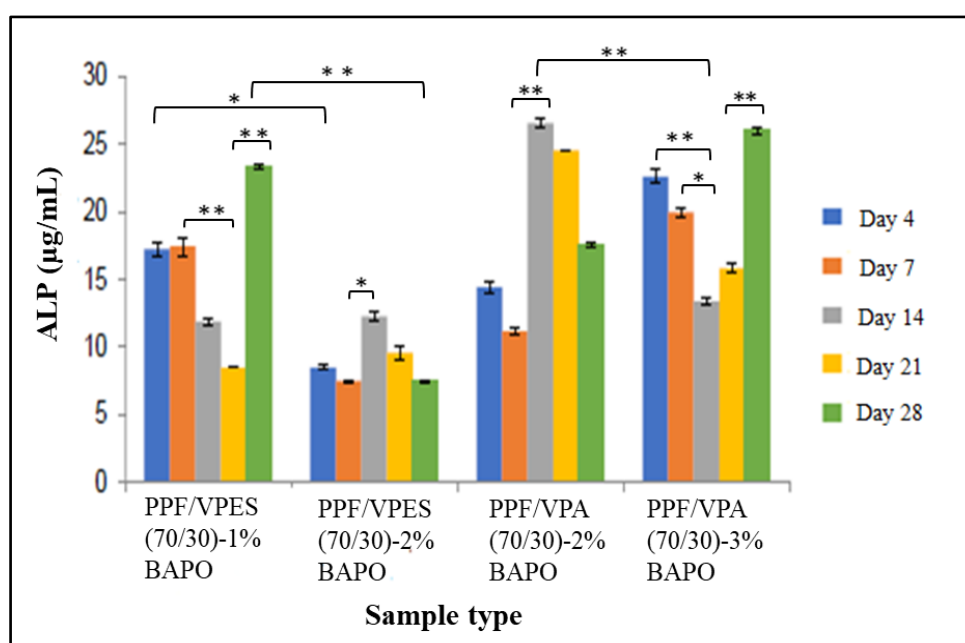


Figure 4.12. ALP activity of HOB cells on UV-cured PPF/VPA (70/30) and PPF/VPES (70/30) samples with different BAPO concentrations. * and ** indicate a significant difference with a $p < 0.05$ and $p < 0.01$, respectively.

Figure 4.13 indicates the ALP activity of HOB cells on BT-cured PPF/VPES (70/30) samples with different β -TCP ratios on day 4, 7, 14, 21, and 28. All samples indicated high ALP activity on day 4. The highest ALP activity was observed on BT-cured PPF/VPES with 0 per cent β -TCP and 5 per cent β -TCP at this day. Although, ALP activity declined significantly during 7 days of incubation ($p < 0.01$), a significant increase was observed between days 14 and 21 ($p < 0.01$) for all BT-cured samples. After 21 days of incubation, ALP activity increased significantly for the samples with 10 per cent, 15 per cent, and 20 per cent β -TCP. Although, the samples including 10 per cent and 15 per cent β -TCP ratios indicated a high level of ALP expression on day 28, there was a significant difference between sample with 15 per cent β -TCP and other BT-cured samples in terms of ALP activity on day 28 ($p < 0.01$). Therefore, adhered HOB cells tended to differentiate and express more ALP on samples including 5 per cent and 15 per cent β -TCP compared to other VPES samples.

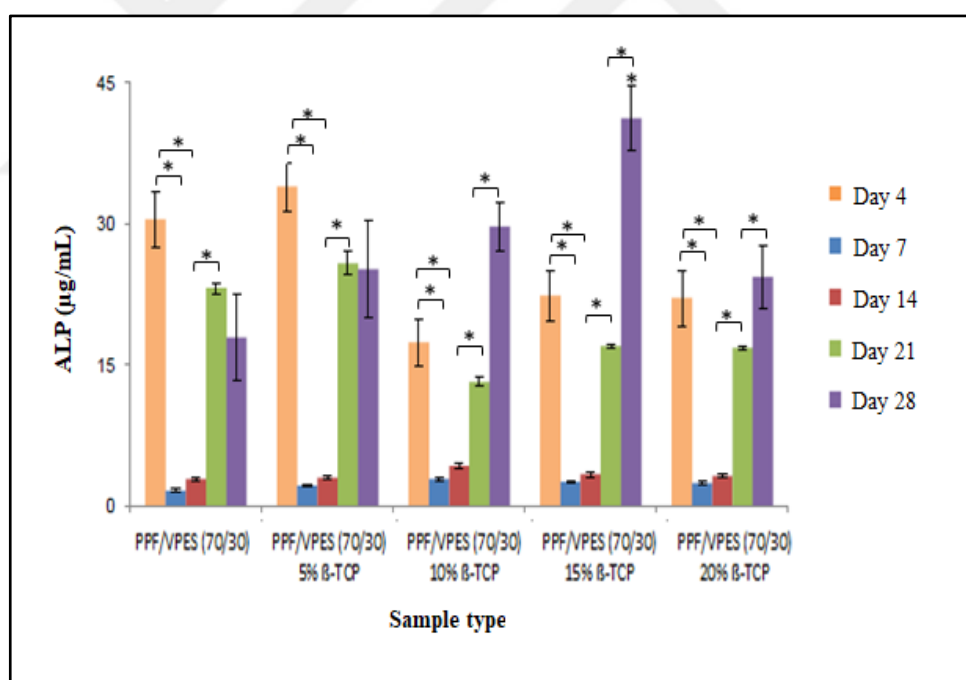


Figure 4.13. ALP activity of HOB cells on BT-cured PPF/VPES (70/30) samples and its composites with different β -TCP ratios. * indicate a significant difference with a $p < 0.01$.

4.1.5. Osteocalcin Assay

Osteocalcin activity of cells on samples was determined throughout 28 days of incubation. The calibration curve of osteocalcin assay can be seen in Appendix B. Since it is the late marker, OC activity was very low in HOb cells on day 7 for all UV-cured PPF samples (Figure 4.14). It was observed that OC activity increased with increasing incubation time for all UV-cured PPF samples.

OC activity of HOb cells on UV-cured PPF/VPA sample including 2 per cent BAPO increased throughout 28 days of incubation, but this increase was significant only between day 21 and day 28 ($p < 0.05$). A significant increase was observed only for PPF/VPA (70/30) including 3 per cent BAPO on day 14 ($p < 0.01$). This increase continued between days 14 and 28 ($p < 0.01$).

For UV-cure PPF/VPES samples, OC activity increased significantly on day 21 and day 28. There was no significant difference between UV-cured VPES samples. In other respects, there was a significant difference between UV-cured PPF/VPA sample with 3 per cent BAPO and other UV-cured samples on day 14 and 28 in terms of OC activity. Also, the highest OC expression was measured for the sample including 3 per cent BAPO on day 28 and this sample was the most suitable sample among all UV-cured samples with respect to cell differentiation.

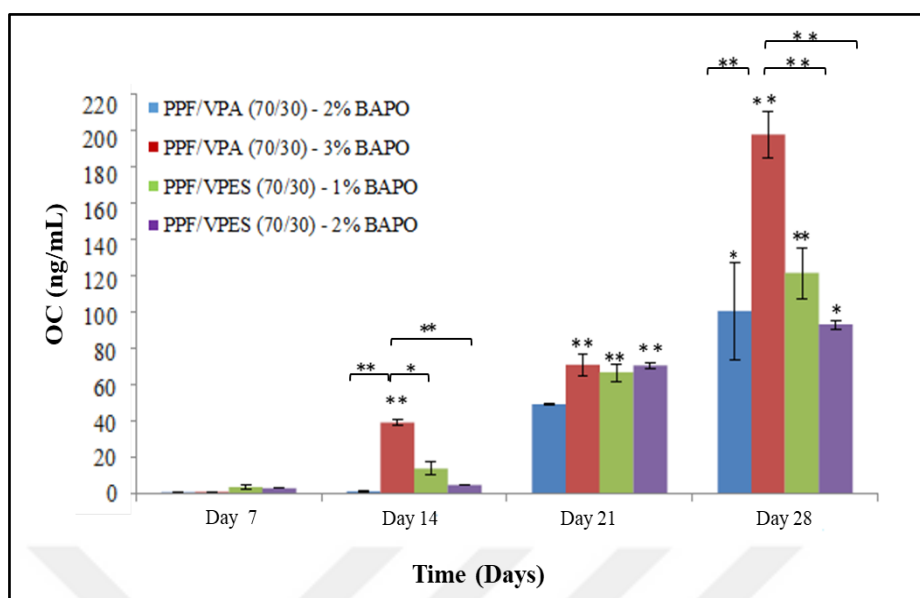


Figure 4.14. OC activity of HOB cells on UV-cured PPF/VPA (70/30) and PPF/VPES (70/30) samples with different BAPO concentrations. * and ** indicate a significant difference with a $p < 0.05$ and $p < 0.01$, respectively.

Figure 4.15 showed the OC activity of HOB cells on BT-cured PPF/VPES (70/30) samples with different β -TCP ratios on day 7, 14, 21, and 28. All samples indicated higher OC activity after 14 days of incubation and this increase was significant. Also, a significant increase was observed between days 21 and 28 for all BT-cured samples. When we compare the BT-cured samples, 0 per cent and 10 per cent β -TCP including samples indicated a high level of OC expression on day 21 and 28 and this difference was significant ($p < 0.01$). Therefore, these samples were the most suitable sample among all BT-cured samples with respect to cell differentiation.

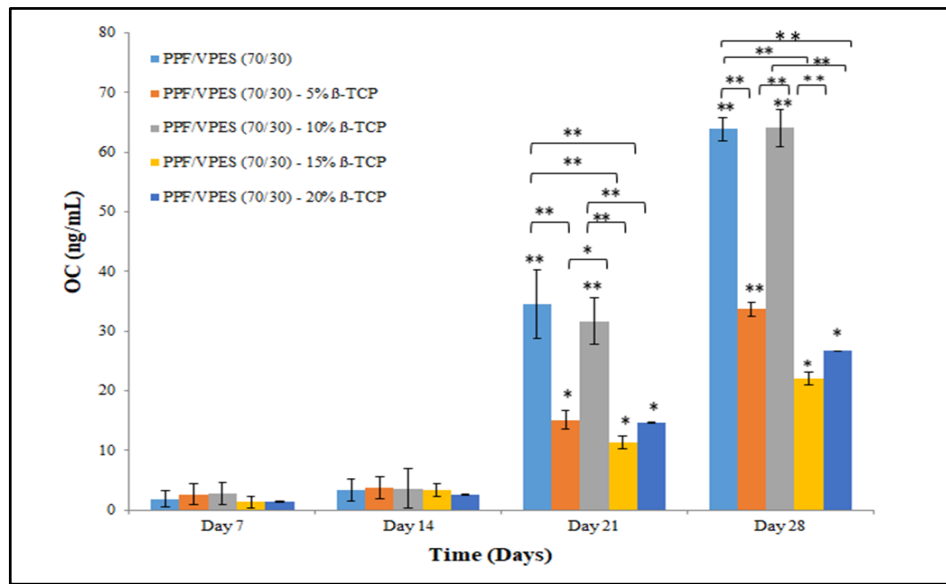


Figure 4.15. OC activity of HOB cells on BT-cured PPF/VPES (70/30) samples and its composites with different β -TCP ratios. * and ** indicate a significant difference with a $p < 0.05$ and $p < 0.01$, respectively.

5. DISCUSSION

Advanced BTE applications should provide well designed scaffold systems with suitable osteoinductivity and osteoconductivity for favorable cell attachment, proliferation, growth, and differentiation. Also, it should provide a porous structure for cell recruitment, nutrient and waste transport. In most of the BTE studies, PPF has been commonly preferred polymers because of its safety, biocompatibility, and good mechanical properties [98]. In addition, PPF has many advantages when compared to other synthetic polymers such as its cross-linking property, using as an injectable scaffold, and allowing for direct application into a defect site [114]. It was also shown that cross-linked PPF scaffolds are able to support bone formation in many studies [98, 106, 107]. All of these studies demonstrated that PPF based scaffolds have crucial potential to promote bone regeneration. In the current study, we aimed to examine the role of PPF/VPA and PPF/VPES based novel scaffolds in *in vitro* bone regeneration. For this purpose, we firstly determined the potentials of UV cured PPF/VPA and PPF/VPES scaffolds in the presence of two different BAPO concentrations for TE. Secondly, the effects of BT cured PPF/VPES and PPF/VPES- β -TCP based scaffolds, and different β -TCP concentrations on HOOb cells biocompatibility, initial cell attachment, mineralization, ALP activity, and OC activity were investigated.

In this study, HOOb cell line was used to test the biocompatibility of the scaffolds since they are used as an excellent model system in most of the BTE studies [115, 116, 117]. *In vitro* and *in vivo* HOOb cell differentiation can be determined in three stages which are cell proliferation, ECM maturation, and ECM mineralization. For *in vitro* studies, ECM maturation and mineralization are generally improved by culturing cells in osteogenic medium after 3 days of incubation [118, 119]. At the first stage which is a cell proliferation stage, ECM proteins can be detected. In matrix maturation stage, HOOb cells express OC, BSP, OPN. Also, at the end of this stage, mineralization is completed and it can be observed using suitable staining (i.e. von Kossa staining) procedures. Therefore, HOOb cells was preferred in this study to indicate the role of bone formation capacity of PPF based scaffolds. Moreover, rapid proliferation rate and differentiation capacity made HOOb cells preferable in this study.

The first part of this study included the preparation of PPF based scaffolds in different comonomer contents (VPA-VPES) and cure types (UV-cure and BT-cure). In this part, UV-

cured samples including different BAPO concentrations were cured successfully. On the other hand, there was a problem during BT curing of samples in which BP was used as a crosslinker. PPF/VPA polymers could not be cured at BT. Timmer *et al.* revealed that BAPO (photo-initiator) is more effective initiator substance than BP (chemical initiator) since crosslinking with BAPO provides higher conversion of double bonds with respect to BP [120]. Accordingly, it may be the reason of unsuccessful cure of PPF/VPA polymers in BT in which BP was used as a crosslinker. In spite of unsuccessful cure of VPA, PPF/VPES polymers were able to get cured at BT. It could be due to the higher reactivity of VPES with respect to VPA.

Since the usage of BT-cured scaffolds provide many advantages such as easy handling, time saving procedure, etc. especially during *in vivo* implantation, we tried to improve their physical properties by making a composite of PPF/VPES and β -TCP. Similarly in other studies, PPF was combined with β -TCP to encourage bone ingrowth and create a porous scaffold which possesses sufficient mechanical features [121, 122]. It was revealed that these composite scaffolds maintain the desired mechanical features over several weeks both *in vitro* and *in vivo* studies.

The morphology of HOB cells that were seeded on UV-cured and BT-cured PPF based scaffolds were examined by using SEM. This examination allows to observe HOB cell attachment, spreading, and proliferation on the different types of PPF scaffold surfaces. In this study, HOB cells attached and spread out to the edge of rough scaffold surfaces except UV-cured PPF/VPA. In that type of scaffold, cells attached and penetrated inside the scaffold. This penetration was related with swelling and softening of these samples in osteogenic media since UV-cured PPF/VPA samples were more hydrophilic than PPF/VPES samples. All cells on the scaffolds formed bridging orthogonal filopodia and ECM throughout a 28 days of incubation. It was too important since ECM formation not only provides structural support for the cell attachment, growth, proliferation, and differentiation but also provides biological cues to regulate cell activities [123]. Similarly, Farshid *et al.* observed the effects of ECM matrix formation of MC3T3 pre-osteoblasts on the surface of PPF based nanocomposites that was crosslinked with N-vinyl pyrrolidone [124].

Cell proliferation assay was the most important step in *in vitro* examination of PPF based samples. In order to observe cell proliferation and attachment, MTS cell viability assay

was used. MTS solution (3-(4,5-dimethylthiazol-2-yl)-5-(3-carboxymethoxy phenyl)-2-(4-sulfophenyl)-2H-tetrazolium) includes tetrazolium reagents that is used with intermediate electron acceptor reagents such as phenazine methyl sulfate and phenazine ethyl sulfate. This MTS solution is reduced by metabolically active cells into a soluble formazan product. The absorbance value of this product reflects the number of viable cells in culture [125]. MTS cell proliferation assay demonstrated that both UV-cured and BT-cured PPF based scaffolds had not cytotoxic effects on HOOb cells and supported cell attachment and proliferation. Gemeinhart *et al.* demonstrated that VPA based scaffolds in BTE studies supported osteoblast cell attachment, growth, and proliferation [126]. Therefore, it was an expected result of observing high number of viable cells on UV-cured PPF/VPA samples compared to PPF/VPES samples and only cell containing group. Moreover, according to characterization studies, VPA samples were more hydrophilic than VPES samples. Therefore, initial cell attachment on PPF/VPA was better than that of PPF/VPES scaffolds. Additionally, all BT-cured samples had similar initial cell attachment and proliferation pattern. All samples indicted a peak on day 21 and after that day HOOb cell number decreased. This decline could be the differentiation of HOOb cells. This study also indicated that different β -TCP ratios had no effect on HOOb cell proliferation. Similarly, Petrovic *et al.* showed that none of the β -TCP composites with different ratios supported cell proliferation of osteoblasts when compared to control group [127]. Moreover, β -TCP addition not only increases mechanical properties of the scaffolds (i.e. tensile strength, elastic modulus) but also increases the hydrophilicity due to higher contents of phosphate groups [124, 125, 128]. Accordingly, PPF/VPES- β -TCP composites had higher viable HOOb cell number compared to PPF/VPES scaffolds without β -TCP at the end of 28 days of incubation.

Mineralization is the late-marker of osteogenesis and commonly visualized by Von Kossa staining. This staining contains the precipitation reaction where silver ions react with phosphate forming black regions [129]. Therefore, calcium phosphate deposits (calcification) can be seen easily with naked eye when the cell culture layer is stained with Von Kossa. While black region is the indicator of calcified ECM, red region indicates the nucleus, and light pink region indicates the cytoplasm [130]. It was revealed that fourteen days of incubation is a sufficient time to observe positive staining since mineralization is the late-marker of new bone tissue formation [131]. Similarly, according to von Kossa

staining results of this study, after 14 days of incubation all samples indicated positive staining except the UV-cured PPF/VPES sample containing 2 per cent BAPO. This could be due to the proliferation of cells on UV-cured PPF/VPES instead of differentiation. MTS results also showed that after 14 days of incubation, there was a cell proliferation on UV-cured PPF/VPES scaffolds with 2 per cent BAPO. Correlated with the MTS results, there was no significant difference between two UV-cured PPF/VPA samples and these samples supported mineralization better than PPF/VPES samples. Additionally, Qi *et al.* indicated that β -TCP had a positive effect on mineralization of mice osteoblasts [132]. Also, results of Color Pic. software analysis in which lower values indicate higher mineralization showed that BT-cured samples were less than UV-cured samples. Therefore, we can say that BT-cured samples supported mineralization and osteogenesis better than UV-cured samples. Besides, the darkest color was recorded for BT-cured PPF/VPES sample including 0 per cent and 15 per cent β -TCP but the values of the samples were very close to each other.

ALP activity is widely used early marker for osteogenesis, because it is associated with the proportion of osteogenically differentiated cells. ALP is an ubiquitous enzyme which reduces phosphate-including compounds and produces free phosphates for regulating the mineralization process. ALP activity was determined with using the substrate of ALP enzyme which is *p*-nitrophenylphosphate. It is converted into yellow colored product, *p*-nitrophenol [133]. The absorbance value at 405 nm of this product reflects the amount of produced ALP enzyme by HOB cells. Since ALP activity is cyclic which means its activity increasing and decreasing periodically in the cell, variable ALP activity of the HOB cells was an expected result throughout 28 days of incubation. All samples indicated the early stages of osteogenesis and showed higher ALP activity on day 4. Therefore, this high level of ALP activity reflected the newly proliferated and differentiated HOB cells on day 4. Moreover, Li *et al.* revealed that intercellular communication has an important effect on expression of differentiation markers in osteoblasts. Higher cell density leads to higher cellular interactions and so higher differentiation rate [134]. In accordance with this information, ALP assay results and MTS assay results supported each other. Correlated with the MTS assay, there was no significant difference between two UV-cured PPF/VPA samples and UV-cured PPF/VPES samples supported osteogenesis better than UV-cured PPF/VPES samples. In another study, the function of marrow stromal cells on PPF/ β -TCP

composites was investigated. The results of ALP assay of this study indicated a higher ALP expression on day 21 and 28. Similarly in this study, all BT-cured composites showed higher ALP activity on day 28. However, BT-cured PPF/VPES composites with 0 per cent and 5 per cent β -TCP promoted osteoblast differentiation better than other BT-cured samples and these samples were selected as suitable scaffolds according to ALP assay results.

OC is a non-collagen bone Gla-protein which is the most commonly used late marker for osteogenesis. It is secreted after the other osteoblastic markers such as ALP and type I collagen. OC binds to HA via three carboxylated Gla residues. Its concentration increases with time when there is an increased activity of bone formation [26]. Therefore, similarly in ALP, it indicates the proportion of osteogenically differentiated cells. Since OC is the late marker, it was expected that all UV-cured and BT-cured samples showed low OC expression throughout 14 days of incubation. As it was mentioned before, when proliferation rate of the osteoblasts decreases, cells began to express osteoblastic markers [135]. Therefore, we can conclude that increasing OC activity after 14 days of incubation indicated the differentiation of HOb cells. Similarly, Peter *et al.* showed significant increase of OC activity after 14 days of incubation on PPF/ β -TCP composites [116]. The results of this study indicated that UV-cured PPF/VPA sample including 3 per cent BAPO supported OC activity better than other UV-cured samples. Moreover, BT-cured PPF/VPES sample without β -TCP and composites with 10 per cent β -TCP indicated higher OC expression on day 28. Therefore, adhered HOb cells tended to differentiate and express more OC on these samples.

In accordance with these researches and results of this study, we can conclude that both UV-cured and BT-cured PPF based scaffold systems were biocompatible. Also they provided an osteoconductive surface, and supported HOb cells attachment, proliferation, and differentiation. Additionally, we can conclude that UV-cured PPF/VPA samples supported osteogenesis better than PPF/VPES samples. Among BT-cured samples, PPF/VPES samples with 0 and 10 per cent β -TCP were selected as a suitable scaffold according to all assay results. This study also revealed that PPF/VPA and PPF/VPES scaffold systems have promising features for BTE applications.

6. CONCLUSION

The main purpose of this study was to determine the role of PPF/VPA and PPF/VPES based novel scaffolds in bone regeneration. For that purpose, at the first part of scaffold preparation, PPF was cured in the presence of two phosphonic acid co-monomers, VPA and VPES, at 70/30 ratio in the presence of 2 per cent and 3 per cent BAPO. At the second part of the scaffold preparation, PPF was cured with VPES co-monomer at 37°C. At the last part, composites of this PPF/VPES polymer system were prepared with using different ratios of β -TCP. It was observed that all of these scaffolds were cured successfully. For *in vitro* studies HOB cells were used to determine the biocompatibility of these UV-cured and BT-cured scaffold systems. SEM results demonstrated that HOB cells were able to attach and spread on all sample types while maintaining their osteoblastic morphology. Cell proliferation assay indicated that initial cell attachment was similar between each type of UV-cured samples but PPF/VPA samples supported cell proliferation better than PPF/VPES samples. Also, MTS assay revealed that different β -TCP ratios had no significant effect on cell proliferation. Von Kossa staining results demonstrated that UV-cured PPF/VPA samples promoted mineralization better than PPF/VPES samples. Also, all BT-cured samples with and without β -TCP indicated largely mineralized regions. Furthermore, ALP assay results revealed that PPF/VPA scaffolds supported osteogenesis better than the PPF/VPES scaffolds and the highest ALP activity was recorded for samples with 0 per cent and 5 per cent β -TCP among BT-cured PPF/VPES samples. Finally, UV-cured PPF/VPA sample with 3 per cent BAPO indicated highest OC activity with respect to other UV-cured samples. Also, BT-cured PPF/VPES without and with 10 per cent β -TCP promoted osteogenesis better than other BT-cured samples.

To conclude, UV-cured PPF/VPA and PPF/VPES and BT-cured PPF/VPES and PPF/VPES- β -TCP composites were biocompatible and promote HOB cell attachment, proliferation, growth, and differentiation. Among these scaffolds, UV-cured PPF/VPA samples with 3 per cent BAPO, BT-cured PPF/VPES without and with 10 per cent β -TCP samples have a great potency for BTE applications. Also, BT-cured PPF/VPES- β -TCP composites can be preferred in injectable form as a scaffold for cartilage tissue regeneration.

7. FUTURE PROSPECTS

The results of this study gave crucial insights about the potential applications of UV-cured and BT-cured PPF based scaffolds for bone formation. However, UV-cured and BT-cured PPF based scaffolds should be examined further. For instance, both UV-cured scaffold types can be combined with β -TCP to improve the physical properties of scaffolds. Moreover, *in vitro* and *in vivo* studies can be performed to investigate the potential of these composites for BTE applications.

Real time PCR analysis should be done to identify up-regulated and down-regulated genes in bone formation such as collagen type I, ALP, OC, OSP, and etc. *In vitro* studies are not sufficient to reflect the actual effect of the scaffolds and actual response of the body. Therefore, *in vivo* studies should be performed to test the functionality of the designed polymer systems in terms of bone regeneration and inflammatory response.

Different amino acid chains can also be added at the end of PPF polymer chain to enhance the initial cell attachment onto these scaffolds. Additionally, these scaffolds have a good potential to be used as a drug delivery systems. The release kinetics of BMP can be studied with these polymer systems to induce osteogenic differentiation.

REFERENCES

1. Lowe JS, Anderson PG. *Human Histology*. Philadelphia: Mosby; 2015.
2. Gartner LP, Hiatt JL. *Color Atlas of Histology*. Philadelphia: Lippincott Williams and Wilkins; 2006.
3. Clarke B. Normal bone anatomy and physiology. *Clin J Am Soc Nephrol*. 2008;3(3):131–9.
4. Doblaré M, García JM, Gómez MJ. Modelling bone tissue fracture and healing: A review. *Eng Fract Mech*. 2004;71(13–14):1809–40.
5. Long M, Rack HJ. Titanium alloys in total joint replacement--a materials science perspective. *Biomaterials*. 1998;19(18):1621–39.
6. Meier DE, Orwoll ES, Jones JM. Marked disparity between trabecular and cortical bone loss with age in healthy men: Measurement by vertebral computed tomography and radial photon absorptiometry. *Ann Intern Med*. 1984;101(5):605–12.
7. Hill PA. Bone remodelling. *Br J Orthod*. 1998;25(2):101–7.
8. Porter JR, Ruckh TT, Popat KC. Bone tissue engineering: A review in bone biomimetics and drug delivery strategies. *Biotechnol Prog*. 2009;25(6):1539–60.
9. Osaka A, Miura Y, Takeuchi K, Asada M, Takahashi K. Calcium apatite prepared from calcium hydroxide and orthophosphoric acid. *J Mater Sci Mater Med*. 1991;2(1):51–5.
10. Lazar T, Tres L. *Histology and Cell Biology—An Introduction to Pathology*, St. Louis, MO, USA: Mosby Publishers; 2002.
11. Wegst UGK, Bai H, Saiz E, Tomsia AP, Ritchie RO. Bioinspired structural materials. *Nat Mater*. 2015;14(1):23–36.
12. Kogianni G, Noble BS. The biology of osteocytes. *Curr Osteoporos Rep*. 2007;5(2):81–6.

13. Miller SC, de Saint-Georges L, Bowman BM, Jee WS. Bone lining cells: Structure and function. *Scanning Microsc.* 1989;3(3):953-60.
14. Islam A, Glomski C, Henderson ES. Endothelial cells and hematopoiesis: A light microscopic study of fetal, normal, and pathologic human bone marrow in plastic-embedded sections. *Anat Rec.* 1992;233(3):440–52.
15. Boyce BF, Yao Z, Zhang Q, Guo R, Lu Y, Schwarz EM, et al. New roles for osteoclasts in bone. *Ann N Y Acad Sci.* 2007;1116:245–54.
16. Lorenzo JA. Do osteoclasts have dual roles: Bone resorption and antigen presentation? *IBMS Bonekey.* 2011;8(1):37–40.
17. Murphy G, Reynolds JJ. Extracellular matrix degradation. *Connective tissue and its heritable disorders: Molecular, Genetic, and Medical Aspects.* 2002:343–84.
18. Neutzsky-Wulff AV, Sørensen MG, Kocijancic D, Leeming DJ, Dziegiel MH, Karsdal MA, et al. Alterations in osteoclast function and phenotype induced by different inhibitors of bone resorption-implications for osteoclast quality. *BMC Musculoskelet Disord.* 2010;11:109.
19. Tanaka Y, Nakayamada S, Okada Y. Osteoblasts and osteoclasts in bone remodeling and inflammation. *Current Drug Targets - Inflammation & Allergy.* 2005;4:325–8.
20. Langdahl B, Ferrari S, Dempster DW. Bone modeling and remodeling: potential as therapeutic targets for the treatment of osteoporosis. *Ther Adv Musculoskelet Dis.* 2016;8(6):225–35.
21. Manolagas SC. Cell number versus cell vigor—what really matters to a regenerating skeleton? *Endocrinology.* 1999;140(10):4377–81.
22. Raisz LG. Physiology and pathophysiology of bone remodeling. *Clin Chem.* 1999;45:1353–8.
23. Dodds RA, Connor JR, James IE, Lee Rykaczewski E, Appelbaum E, Dul E, et al. Human osteoclasts, not osteoblasts, deposit osteopontin onto resorption surfaces: An in vitro and ex vivo study of remodeling bone. *J Bone Miner Res.*

- 1995;10(11):1666–80.
24. Vaes G. Cellular biology and biochemical mechanism of bone resorption: A review of recent developments on the formation, activation, and mode of action of osteoclasts. *Clinical Orthopaedics and Related Research*. 1988;231:239-271.
 25. Cowles EA, DeRome ME, Pastizzo G, Brailey LL, Gronowicz GA. Mineralization and the expression of matrix proteins during in vivo bone development. *Calcif Tissue Int*. 1998;62(1):74–82.
 26. Ivaska KK, Hentunen TA, Vääräniemi J, Ylipahkala H, Pettersson K, Väänänen HK. Release of intact and fragmented osteocalcin molecules from bone matrix during bone resorption in vitro. *J Biol Chem*. 2004;279(18):18361–9.
 27. Beck GR. Inorganic phosphate as a signaling molecule in osteoblast differentiation. *J Cell Biochem*. 2003;90(2):234–43.
 28. Anderson HC, Hsu HH, Morris DC, Fedde KN, Whyte MP. Matrix vesicles in osteomalacic hypophosphatasia bone contain apatite-like mineral crystals. *Am J Pathol*. 1997;151(6):1555–61.
 29. Eriksen EF, Brixen K, Charles P. New markers of bone metabolism: Clinical use in metabolic bone disease. *Eur J Endocrinol*. 1995;132(3):251–63.
 30. Sase SP, Ganu J V, Nagane N. Osteopontin : A novel protein molecule. *Ind Med Gaz*. 2012:62–6.
 31. Sodek J, Ganss B, McKee MD. Osteopontin. *Crit Rev Oral Biol Med*. 2000;11(3):279–303.
 32. Gerstenfeld LC, Shapiro FD. Expression of bone-specific genes by hypertrophic chondrocytes: Implications of the complex functions of the hypertrophic chondrocyte during endochondral bone development. *J Cell Biochem*. 1996;62(1):1–9.
 33. Maillard C, Malaval L, Delmas PD. Immunological screening of SPARC/Osteonectin in nonmineralized tissues. *Bone*. 1992;13(3):257–64.

34. Guweidhi A, Wentz MN, Giese T, Bu MW. Osteonectin influences growth and invasion of pancreatic cancer cells. *Ann Surg*. 2005;242(2):224–34.
35. Rodríguez IR, Moreira EF, Bok D, Kantorow M. Osteonectin/SPARC secreted by RPE and localized to the outer plexiform layer of the monkey retina. *Invest Ophthalmol Vis Sci*. 2000;41(9):2438–44.
36. Viguet-Carrin S, Garnero P, Delmas PD. The role of collagen in bone strength. *Osteoporos Int*. 2006;17(3):319–36.
37. Schindeler A, McDonald MM, Bokko P, Little DG. Bone remodeling during fracture repair: The cellular picture. *Semin Cell Dev Biol*. 2008;19(5):459–66.
38. Meng KP, E. BJ. Macrophage and dendritic cell phenotypic diversity in the context of biomaterials. *J Biomed Mater Res Part A*. 2010;96(1):239–60.
39. Hing KA. Bone repair in the twenty-first century: biology, chemistry or engineering? *Philos Trans R Soc London Ser A Math Phys Eng Sci*. 2004;362(1825):2821–50.
40. Olivier V, Faucheux N, Hardouin P. Biomaterial challenges and approaches to stem cell use in bone reconstructive surgery. *Drug Discov Today*. 2004;9(18):803–11.
41. Dimitriou R, Jones E, McGonagle D, Giannoudis P. Bone regeneration: Current concepts and future directions. *BMC Med*. 2011;9:66.
42. Betz RR. Limitations of autograft and allograft: New synthetic solutions. *Orthopedics*. 2002;25:561–70.
43. Ladd A, Pliam N, Yao J. Bone graft substitutes in the radius and upper limb. *Journal of the American Society for Surgery of the Hand*. 2003;3(4):227–45.
44. Seiler JG, Johnson J. Iliac crest autogenous bone grafting: Donor site complications. *J South Orthop Assoc*. 2000;9(2):91–7.
45. Benichou G. Direct and indirect antigen recognition: The pathways to allograft immune rejection. *Front Biosci*. 1999;4:D476–80.

46. Langer R, Vacanti JP, Series N, May N. Tissue engineering. *Science*. 1993;260(5110):920–6.
47. Khan WS, Rayan F, Dhinsa BS, Marsh D. An osteoconductive, osteoinductive, and osteogenic tissue-engineered product for trauma and orthopaedic surgery: How far are we? *Stem Cells Int*. 2012;2012.
48. Ikada Y. Challenges in tissue engineering. *Journal of the Royal Society Interface*. 2006;3:589-601.
49. Killian ML, Cavinatto L, Galatz LM, Thomopoulos S. Recent advances in shoulder research. *Arthritis Res Ther*. 2012;14(3):214.
50. Shieh S-J, Vacanti JP. State-of-the-art tissue engineering: From tissue engineering to organ building. *Surgery*. 2005;137(1):1–7.
51. Kneser U, Schaefer DJ, Polykandriotis E, Horch RE. Tissue engineering of bone: the reconstructive surgeon's point of view. *J Cell Mol Med*. 2006;10(1):7–19.
52. McLaren A. A scientist's view of the ethics of human embryonic stem cell research. *Cell Stem Cell*. 2007;1(1):23–6.
53. Kiel MJ, Morrison SJ. Maintaining hematopoietic stem cells in the vascular niche. *Immunity*. 2006;25(6):862–4.
54. Caplan AI. Review: Mesenchymal stem cells: Cell-based reconstructive therapy in orthopedics. *Tissue Eng*. 2005;11(7–8):1198–211.
55. Honda MJ, Imaizumi M, Tsuchiya S, Morsczeck C. Dental follicle stem cells and tissue engineering. *J Oral Sci*. 2010;52(4):541–52.
56. Hart C, Drewel D, Mueller G, Grassinger J, Zaiss M, Kunz-schughart LA, et al. Expression and function of homing-essential molecules and enhanced in vivo homing ability of human peripheral blood-derived hematopoietic progenitor cells after stimulation with stem cell factor. *Stem Cells*. 2004;580–9.
57. Levi B, Longaker MT. Adipose derived stromal cells for skeletal regenerative medicine. *Stem Cells*. 2011;29(4):576–82.

58. Kotaro Y, Tomokuni S, Daisuke M, Takahiro S, Yasuyuki T, Emiko A-K, et al. Characterization of freshly isolated and cultured cells derived from the fatty and fluid portions of liposuction aspirates. *J Cell Physiol*. 2006;208(1):64–76.
59. Kanczler JM. Osteogenesis and angiogenesis : The potential for engineering bone. *Eur Cell Mater*. 2008;15:100–14.
60. Shepherd J, Best S. Calcium phosphate scaffolds for bone repair. *JOM*. 2011;63:83-92.
61. Goustin AS, Leof EB, Shipley GD, Moses HL. Growth factors and cancer. *Cancer Res*. 1986;46(3):1015 LP-1029.
62. Rose FR, Oreffo RO. Bone tissue engineering: hope vs hype. *Biochem Biophys Res Commun*. 2002;292(1):1–7.
63. AI-Aql ZS, Alagl AS, Graves DT, Gerstenfeld LC, Einhorn TA. Molecular mechanisms controlling bone formation during fracture healing and distraction osteogenesis. *J Dent Res*. 2008;87(2):107–18.
64. Biase P De, Capanna R. Clinical applications of BMPs. *Injury*. 2005;36(3):S43–6.
65. Fischer J, Kolk A, Wolfart S, Pautke C, Warnke PH, Plank C, et al. Future of local bone regeneration - Protein versus gene therapy. *J Craniomaxillofac Surg*. 2011;39(1):54–64.
66. Chin HB, Tong C, Walter SL, Paul R, Bjorn O. Strategies for directing the differentiation of stem cells into the osteogenic lineage in vitro. *J Bone Miner Res*. 2009;19(9):1379–94.
67. Fisher JP, Mikos AG, Bronzino JD. *Tissue Engineering*. New York:CRC Press;2006.
68. Rezwan K, Chen QZ, Blaker JJ, Boccaccini AR. Biodegradable and bioactive porous polymer/inorganic composite scaffolds for bone tissue engineering. *Biomaterials*. 2006;27(18):3413–31.
69. Karageorgiou V, Kaplan D. Porosity of 3D biomaterial scaffolds and osteogenesis.

- Biomaterials*. 2005;26(27):5474–91.
70. Badylak SF. The extracellular matrix as a biologic scaffold material. *Biomaterials*. 2007;28(25):3587–93.
 71. Agrawal CM, Ray RB. Biodegradable polymeric scaffolds for musculoskeletal tissue engineering. *J Biomed Mater Res*. 2001;55(2):141–50.
 73. Asadi-Eydivand M, Solati-Hashjin M, Farzad A, Abu Osman NA. Effect of technical parameters on porous structure and strength of 3D printed calcium sulfate prototypes. *Robot Comput Integr Manuf*. 2016;37:57–67.
 74. Engler AJ, Sen S, Sweeney HL, Discher DE. Matrix elasticity directs stem cell lineage specification. *Cell*. 2006;126(4):677–89.
 75. Perry CR. Bone repair techniques, bone graft, and bone graft substitutes. *Clinical orthopaedics and related research*. 1999;360:71-86.
 76. Engh CA, Bobyn JD, Glassman A. Porous-coated hip replacement. The factors governing bone ingrowth, stress shielding, and clinical results. *J Bone Joint Surg. Br*. 1987;69(81):45-55.
 77. Disegi JA, Eschbach L. Stainless steel in bone surgery. *Injury*. 2000;31:D2–6
 78. Uggowitzer PJ, Magdowski R, Speidel MO. Nickel free high nitrogen austenitic steels. *ISIJ Int*. 1996;36(7):901–8.
 79. Liu XY, Chu PK, Ding CX. Surface modification of titanium, titanium alloys, and related materials for biomedical applications. *Mat Sci Eng R*. 2003;47:49-121.
 80. Spoerke ED, Murray NG, Li H, Brinson LC, Dunand DC, Stupp SI. A bioactive titanium foam scaffold for bone repair. *Acta Biomater*. 2005;1(5):523–33.
 81. Pompe W, Worch H, Epple M, Friess W, Gelinsky M, Greil P, et al. Functionally graded materials for biomedical applications. *Materials Science and Engineering: A*. 2003;362:40-60.
 82. Cao W, Hench LL. Bioactive materials. *Ceram Int*. 1996;22(6):493–507.

83. Kim K, Dean D, Lu A, G Mikos A, Fisher J. Early osteogenic signal expression of rat bone marrow stromal cells is Influenced by both hydroxyapatite nanoparticle content and initial cell seeding density in biodegradable nanocomposite scaffolds. *Acta biomaterialia*. 2010;7:1249-1264.
84. Wang H, Li Y, Zuo Y, Li J, Ma S, Cheng L. Biocompatibility and osteogenesis of biomimetic nano-hydroxyapatite/polyamide composite scaffolds for bone tissue engineering. *Biomaterials*. 2007;28:3338-3348.
85. Verret DJ, Ducic Y, Oxford L, Smith J. Hydroxyapatite cement in craniofacial reconstruction. *Otolaryngology Head and Neck Surgery*. 2006;133(6):897-899.
86. Baino F, Vitale-Brovarone C. Bioceramics in ophthalmology. *Acta Biomaterialia*. 2014;10(8):3372-97.
87. Carson J, Bostrom M. Synthetic bone scaffolds and fracture repair. *Injury*. 2007;38:S33-7.
88. Fisher JP, Dean D, Mikos AG. Photocrosslinking characteristics and mechanical properties of diethyl fumarate/poly(propylene fumarate) biomaterials. *Biomaterials*. 2002;23(22):4333-43.
89. Wu KJ, Odom RW. Peer Reviewed: Characterizing synthetic polymers by MALDI MS. *Anal Chem*. 1998;70(13):456A-461A.
90. Yoon DM, Fisher JP. Chondrocyte signaling and artificial matrices for articular cartilage engineering. *Adv Exp Med Biol*. 2006;585:67-86.
91. Furth ME, Atala A. Principles of tissue engineering. *Tissue Engineering:Future Perspectives*. 2014;83-123.
92. Wang S, Lu L, Yaszemski MJ. Bone-tissue-engineering material poly (propylene fumarate): correlation between molecular weight, chain dimensions, and physical properties. *American Chemical Society*. 2008;7(6):1976-82.
93. Diez-Pascual AM. Tissue engineering bionanocomposites based on poly(propylene fumarate). *Polymers (Basel)*. 2017;9(7):1-19.

94. Kasper FK, Tanahashi K, Fisher JP, Mikos AG. Synthesis of poly(propylene fumarate). *Nat Protoc* . 2011;4(4):518–25.
95. Gunatillake PA, Adhikari R, Gadegaard N. Biodegradable synthetic polymers for tissue engineering. *Eur Cells Mater*. 2003;5:1–16.
96. Shung AK, Behravesh E, Jo S, Mikos AG. Crosslinking characteristics of and cell adhesion to an injectable poly(propylene fumarate-co-ethylene glycol) hydrogel using a water-soluble crosslinking system. *Tissue Eng*. 2003;9(2):243–54.
97. Temenoff JS, Kasper FK, Mikos a G. Fumarate-based macromers as scaffolds for tissue engineering applications. *Top Tissue Eng*. 2007;3(713).
98. Westbrook EG. Bone tissue engineering incorporating poly(propylene fumarate) composites: A Mini Review. *Nano Life*. 2016;6:1–10.
99. Shin HJ, Lee J-W, Jung JH, Cho D-W, Lim G. Evaluation of cell proliferation and differentiation on a poly(propylene fumarate) 3D scaffold treated with functional peptides. *Journal of Materials Science*. 2011;46(15):5282-5287.
100. Shung AK, Timmer MD, Jo S, Engel PS, Mikos AG. Kinetics of poly(propylene fumarate) synthesis by step polymerization of diethyl fumarate and propylene glycol using zinc chloride as a catalyst. *J Biomater Sci Polym Ed*. 2002;13(1):95–108.
101. Cai ZY, Yang DA, Zhang N, Ji CG, Zhu L, Zhang T. Poly(propylene fumarate)/(calcium sulphate/ β -tricalcium phosphate) composites: Preparation, characterization and in vitro degradation. *Acta Biomater*. 2009;5(2):628–35.
102. Fang Z, Giambini H, Zeng H, Camp JJ, Dadsetan M, Robb RA, et al. Biomechanical evaluation of an injectable and biodegradable copolymer P(PF-co-CL) in a cadaveric vertebral body defect model. *Tissue Eng Part A*. 2014;20(5–6):1096–102.
103. Zheng X, Bi C, Brooks M, Hage DS. Analysis of Hormone-Protein Binding in solution by ultrafast affinity extraction: interactions of testosterone with human serum albumin and sex hormone binding globulin. *Anal Chem*. 2015;87(22):11187–94.

104. Behravesh E, Mikos AG. Three-dimensional culture of differentiating marrow stromal osteoblasts in biomimetic poly(propylene fumarate-co-ethylene glycol)-based macroporous hydrogels. *J Biomed Mater Res - Part A*. 2003;66(3):698–706.
105. Timmer MD, Carter C, Ambrose CG, Mikos AG. Fabrication of poly(propylene fumarate)-based orthopaedic implants by photo-crosslinking through transparent silicone molds. *Biomaterials*. 2003;24(25):4707–14.
106. Fisher JP, Lalani Z, Bossano CM, Brey EM, Demian N, Johnston CM, et al. Effect of biomaterial properties on bone healing in a rabbit tooth extraction socket model. *J Biomed Mater Res A*. 2004;68(3):428–38.
107. Vehof JWM, Fisher JP, Dean D, van der Waerden J-PCM, Spauwen PHM, Mikos AG, et al. Bone formation in transforming growth factor beta-1-coated porous poly(propylene fumarate) scaffolds. *J Biomed Mater Res*. 2002;60(2):241–51.
108. Lee KW, Wang S, Yaszemski MJ, Lu L. Physical properties and cellular responses to crosslinkable poly(propylene fumarate)/hydroxyapatite nanocomposites. *Biomaterials*. 2008;29(19):2839–48.
109. Sannigrahi A, Takamuku S, Jannasch P, Sannigrahi A, Takamuku S, Jannasch P. Block selective grafting of poly (vinylphosphonic acid) from aromatic multiblock copolymers for nanostructured electrolyte membranes. *Hal*. 2013;4207-18.
110. Schöller K, Ethirajan A, Zeller A, Landfester K. Biomimetic route to calcium phosphate coated polymeric nanoparticles: Influence of different functional groups and pH^a. *Macromol Chem Phys*. 2011;212:1165-1175.
111. Greish Y, Brown PW. Chemically formed HAp-Ca poly(vinyl phosphonate) composites. *Biomaterials*. 2001;22:807-816.
112. Greish YE, Brown PW. Formation and properties of hydroxyapatite–calcium poly(vinyl phosphonate) composites. *J Am Ceram Soc*. 2004;85(7):1738–44.
113. Suwandi JS, Toes REM, Nikolic T, Roep BO. Inducing tissue specific tolerance in autoimmune disease with tolerogenic dendritic cells. *Clin Exp Rheumatol*. 2015;33:97–103.

114. Hedberg EL, Shih CK, Lemoine JJ, Timmer MD, K. Liebschner MA, Jansen JA, et al. In vitro degradation of porous poly(propylene fumarate)/poly(dl-lactic-co-glycolic acid) composite scaffolds. *Biomaterials*. 2005;26(16):3215–25.
115. Mikos AG, Holland TA, Fisher JP, Jansen JA, van der Waerden JPCM, Vehof JWM, et al. Soft and hard tissue response to photocrosslinked poly(propylene fumarate) scaffolds in a rabbit model. *J Biomed Mater Res*. 2002;59(3):547–56.
116. Peter SJ, Lu L, Kim DJ, Mikos AG. Marrow stromal osteoblast function on a poly(propylene fumarate)/ β -tricalcium phosphate biodegradable orthopaedic composite. *Biomaterials*. 2000;21(12):1207–13.
117. Sun JS, Tsuang YH, Liao CJ, Liu HC, Hang YS, Lin FH. The effects of calcium phosphate particles on the growth of osteoblasts. *J Biomed Mater Res*. 1997;37(3):324–34.
118. Correia TR, Figueira DR, de Sá KD, Miguel SP, Fradique RG, Mendonça AG, et al. 3D Printed scaffolds with bactericidal activity aimed for bone tissue regeneration. *Int J Biol Macromol*. 2016;93:1432–45.
119. Kasperk C, Wergedal J, Strong D, Farley J, Wangerin K, Gropp H, et al. Human bone cell phenotypes differ depending on their skeletal site of origin. *J Clin Endocrinol Metab*. 1995;80(8):2511–7.
120. Timmer MD, Ambrose CG, Mikos AG. Evaluation of thermal- and photocrosslinked biodegradable poly(propylene fumarate)-based networks. *J Biomed Mater Res A*. 2003;66(4):811–8.
121. Yaszemski MJ, Payne RG, Hayes WC, Langer RS, Aufdemorte TB, Mikos AG. The ingrowth of new bone tissue and initial mechanical properties of a degrading polymeric composite scaffold. *Tissue Eng*. 1995;1(1):41–52.
122. Peter SJ, Nolley JA, Widmer MS, Merwin JE, Yaszemski MJ, Yasko AW, et al. In vitro degradation of a poly(propylene fumarate)/ β -Tricalcium phosphate composite Orthopaedic Scaffold. *Tissue Eng*. 1997;3(2):207–15.
123. Chan BP, Leong KW. Scaffolding in tissue engineering: general approaches and

- tissue-specific considerations. *Eur Spine J*. 2008;17(Suppl 4):467–79.
124. Farshid B, Lalwani G, Sitharaman B. In vitro cytocompatibility of one-dimensional and two-dimensional nanostructure-reinforced biodegradable polymeric nanocomposites. *J Biomed Mater Res A*. 2015;103(7):2309–21.
 125. Riss TL, Moravec RA, Niles AL, Duellman S, Benink HA, Worzella TJ, et al. Cell viability assays. *Assay Guid Man*. 2013;114(8):785–96.
 126. Gemeinhart RA, Bare CM, Haasch RT, Gemeinhart EJ. Osteoblast-like cell attachment to and calcification of novel phosphonate-containing polymeric substrates. *J Biomed Mater Res Part A*. 2006;78(3):433–40.
 127. Petrovic L, Pohle D, Münstedt H, Rechtenwald T, Schlegel KA, Rupprecht S. Effect of β TCP filled polyetheretherketone on osteoblast cell proliferation in vitro. *J Biomed Sci*. 2006;13(1):41–6.
 128. Ma F, Chen S, Liu P, Geng F, Li W, Liu X, et al. Improvement of beta-TCP/PLLA biodegradable material by surface modification with stearic acid. *Mater Sci Eng C Mater Biol Appl*. 2016;62:407–13.
 129. Brauer A, Pohlemann T, Metzger W. Osteogenic differentiation of immature osteoblasts: Interplay of cell culture media and supplements. *Biotech Histochem*. 2016;91(3):161–9.
 130. Shima WN, Ali AM, Subramani T, Alitheen NBM, Hamid M, Samsudin AR, et al. Rapid growth and osteogenic differentiation of mesenchymal stem cells isolated from human bone marrow. *Exp Ther Med*. 2015;9(6):2202–6.
 131. A. AM, C. GL, A. OT, S. TM, S. SG, B. LJ. Factors that promote progressive development of the osteoblast phenotype in cultured fetal rat calvaria cells. *J Cell Physiol*. 2018;143(2):213–21.
 132. Qi Z, Zhang Q, Zheng Q, Dai H, Wang Z, Qiu M, et al. Effects of β -TCP ceramics on osteoblast cellular proliferating, mineralization and osteocalcin expression. *J Wuhan Univ Technol Sci Ed*. 2012;27(1):107–9.

133. Sabokbar A, Millett PJ, Myer B, Rushton N. A rapid, quantitative assay for measuring alkaline phosphatase activity in osteoblastic cells in vitro. *Bone Miner.* 1994;27(1):57–67.
134. Li Z, Zhou Z, Yellowley CE, Donahue HJ. Inhibiting gap junctional intercellular communication alters expression of differentiation markers in osteoblastic cells. *Bone.* 1999;25(6):661–6.
135. Ishaug SL, Yaszemski MJ, Bizios R, Mikos AG. Osteoblast function on synthetic biodegradable polymers. *J Biomed Mater Res.* 1994;28(12):1445–53.



APPENDIX A: ALKALINE PHOSPHATASE CALIBRATION CURVE

The standard curve of the ALP activity was determined using *p*-nitrophenylphosphate as the substrate. ALP activity of the HOb cells on UV-cured and BT-cured samples were calculated according to this standard curve (Figure A.1).

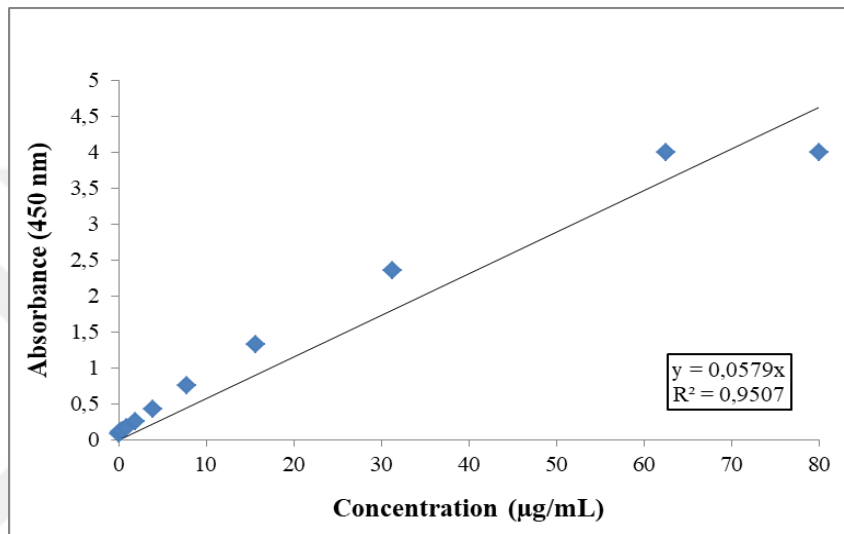


Figure A.1. Calibration curve of ALP assay

APPENDIX B: OSTEOCALCIN CALIBRATION CURVE

The standard curve of the OC activity was determined using standards of human osteocalcin ELISA kit. OC activity of the HOb cells on UV-cured and BT-cured samples were calculated according to this standard curve (Figure B.1)

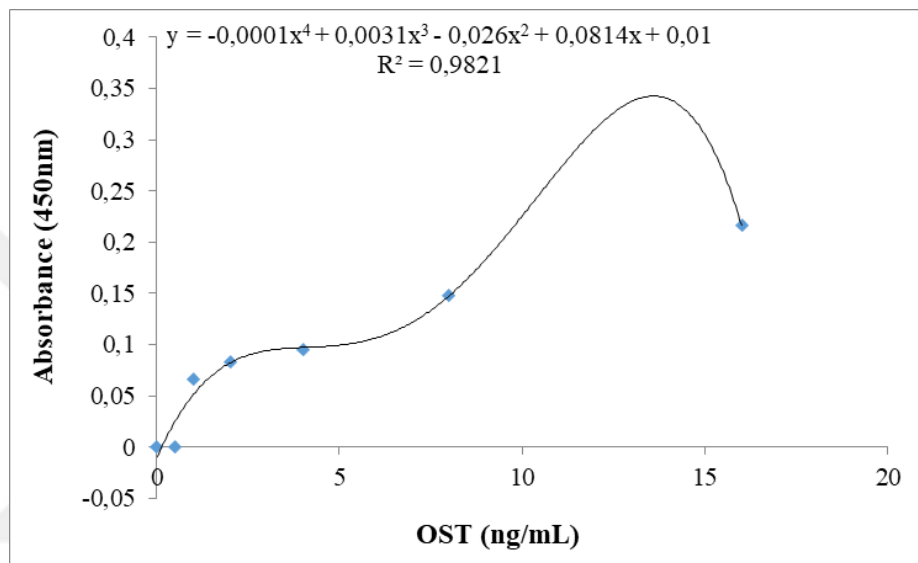


Figure B.1. Calibration curve of OC assay